P-06-91

Forsmark site investigation

Formation factor logging in-situ by electrical methods in KFM05A and KFM06A

Martin Löfgren, Michael Pettersson,
Hans Widén, James Crawford
Kemakta Konsult AB

September 2006

Svensk Kärnbränslehantering AB
Swedish Nuclear Fuel
and Waste Management Co
Box 5864
SE-102 40 Stockholm Sweden
Tel 08-459 84 00
+46 8 459 84 00
Fax 08-661 57 19
+46 8 661 57 19

ISSN 1651-4416
SKB P-06-91

Forsmark site investigation

Formation factor logging in-situ by electrical methods in KFM05A and KFM06A

Martin Löfgren, Michael Pettersson,
Hans Widén, James Crawford
Kemakta Konsult AB

September 2006

Keywords: AP PF 400-05-091, In-situ, Formation factor, Rock resistivity, Electrical conductivity.

Abstract

This report presents measurements and interpretations of the formation factor of the rock surrounding the boreholes KFM05A and KFM06A in Forsmark, Sweden. The formation factor was logged in-situ by electrical methods and is compared to formation factors obtained in the laboratory by electrical methods.

For KFM05A, the in-situ rock matrix formation factors obtained range from 1.1×10^{-5} to 4.5×10^{-4}. The in-situ fractured rock formation factors obtained range from 9.8×10^{-6} to 9.3×10^{-4}. The laboratory (rock matrix) formation factors obtained on drill core samples range from 4.1×10^{-5} to 7.0×10^{-4}. The formation factors appear to be fairly well log-normally distributed. The mean values and standard deviations of the obtained log10-normal distributions are –4.6 and 0.17, –4.6 and 0.21, and –3.8 and 0.29 for the in-situ rock matrix and fractured rock formation factors, and laboratory formation factor, respectively.

For KFM06A, the in-situ rock matrix formation factors obtained range from 1.2×10^{-5} to 1.6×10^{-4}. The in-situ fractured rock formation factors obtained range from 1.2×10^{-5} to 7.1×10^{-4}. No laboratory formation factors were obtained. The formation factors appear to be fairly well log-normally distributed also in this borehole. The mean values and standard deviations of the obtained log10-normal distributions are –4.6 and 0.12 and –4.5 and 0.21 for the in-situ rock matrix and fractured rock formation factor, respectively.

It may be that the rock samples taken from the drill cores and brought to the laboratory are highly altered. The alteration could either be due to de-stressing or to mechanical disturbance induced in the sample preparation. The formation factors obtained in the laboratory may be overestimated by a few factors or even as much as one order of magnitude.

Recently, new matrix pore water chemistry data have been obtained by leaching drill core samples taken from KFM06A. These data support the approach, used in this present report, that the pore water electrical conductivity can be approximated by the electrical conductivity of freely flowing groundwater at a corresponding depth.

Sammanfattning

Denna rapport presenterar mätningar och tolkningar av bergets formationsfaktor runt borrhålen KFM05A och KFM06A i Forsmark, Sverige. Formationsfaktorn har loggats in-situ med elektriska metoder och jämförs med formationsfaktorn erhållen i laboratoriet med elektriska metoder.

För KFM05A varierar den erhållna in-situ formationsfaktorn för bergmatrisen från $1{,}1\times10^{-5}$ till $4{,}5\times10^{-4}$. Den erhållna in-situ formationsfaktorn för sprickigt berg varierar från $9{,}8\times10^{-6}$ till $9{,}3\times10^{-4}$. Den erhållna laborativa formationsfaktorn (för bergmatrisen) varierar från $4{,}1\times10^{-5}$ till $7{,}0\times10^{-4}$. Formationsfaktorn verkar vara någorlunda väl log-normal fördelad. Medelvärdena och standardavvikelserna för de erhållna log10-normal fördelningarna är –4,6 och 0,17, –4,6 och 0,21, samt –3,8 och 0,29 för in-situ formationsfaktorn för bergmatrisen, in-situ formationsfaktorn för sprickigt berg respektive den laborativa formationsfaktorn.

För KFM06A varierar den erhållna in-situ formationsfaktorn för bergmatrisen från $1{,}2\times10^{-5}$ till $1{,}6\times10^{-4}$, medan in-situ formationsfaktorn för sprickigt berg varierar från $1{,}2\times10^{-5}$ till $7{,}1\times10^{-3}$. Inga laborativa formationsfaktorer erhölls. Formationsfaktorn verkar även i detta borrhål vara någorlunda väl log-normal fördelad. Medelvärdena och standardavvikelserna för de erhållna log10-normal fördelningarna är –4,6 och 0,12 för in-situ formationsfaktorn för bergmatrisen samt –4,5 och 0,21 för in-situ formations-faktorn för sprickigt berg.

Det kan vara så att bergproverna tagna från borrkärnorna till laboratoriet är betydligt störda. Störningen kan antingen ha sitt ursprung i avlastning eller i mekanisk påverkan i samband med provförberedning. De erhållna laborativa formationsfaktorerna kan vara överskattade med ett par faktorer eller till och med så mycket som en tiopotens.

Nyligen har nya matrisporvattendata erhållits genom att laka borrkärneprov tagna från KFM06A. Dessa data stödjer tillvägagångssättet som används i denna rapport, där porvattnets elektriska konduktivitet approximeras med hjälp av den elektriska konduktiviteten för fritt flödande vatten på ett motsvarande djup.

Contents

1 Introduction

This document reports the data gained from measurements of the formation factor of rock surrounding the boreholes KFM05A and KFM06A, within the site investigation at Forsmark. The work was carried out in accordance with activity plan AP PF 400-05-091. In Table 1-1 controlling documents for performing this activity are listed. Both activity plan and method descriptions are SKB's internal controlling documents.

The formation factor was logged in-situ by electrical methods. Comparisons are made with formation factors obtained in the laboratory on samples from the drill cores of KFM05A.

Other contractors performed the fieldwork and laboratory work, and that work is outside the framework of this activity. The interpretation of in-situ data and compilation of formation factor logs were performed by Kemakta Konsult AB in Stockholm, Sweden.

Figure 1-1 shows the Forsmark site investigation area and the location of different drill sites. KFM05A and KFM06A are located at the drill sites DS5 and DS6, respectively.

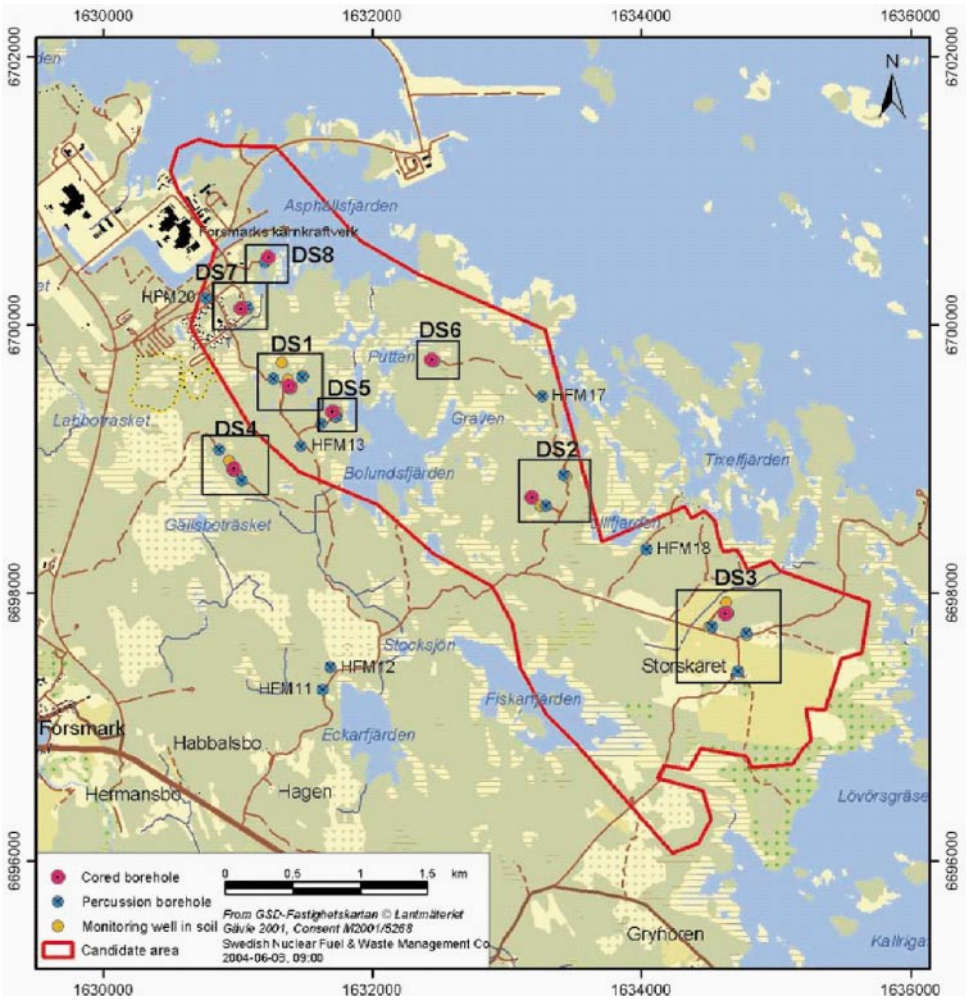

Figure 1-1. *General overview over the Forsmark site investigation area.*

Table 1-1. Controlling documents for performance of the activity.

Activity plan	**Number**	**Version**
Bestämning av formationsfaktorn från in-situ resistivitetsmätningar i KFM05A och KFM06A	AP PF 400-05-091	1.0
Method descriptions	**Number**	**Version**
Bestämning av formationsfaktorn in-situ med elektriska metoder	SKB MD 530.007	1.0

2 Objective and scope

The formation factor is an important parameter that may be used directly in the safety assessment for calculation of radionuclide transport in crystalline rock. The main objective of this work is to obtain the formation factor of the rock mass surrounding the boreholes KFM05A and KFM06A. This has been achieved by performing formation factor loggings by electrical methods both in-situ and in the laboratory. The in-situ method gives a great number of formation factors obtained under more natural conditions than in the laboratory. To obtain the in-situ formation factor, results from previous loggings were used. The laboratory formation factor was obtained by performing measurements on rock samples from the drill core of KFM05A. Other contractors carried out the fieldwork and laboratory work.

3 Equipment

3.1 Rock resistivity measurements

The resistivity of the rock surrounding the boreholes KFM05A /1/ and KFM06A /2/ was logged in two separate campaigns using the focused rock resistivity tool Century 9072. The tool emits an alternating current perpendicular to the borehole axis from a main current electrode. The shape of the current field is controlled by guard electrodes. By using a focused tool, the disturbance from the borehole is minimised. The quantitative measuring range of the Century 9072 tool is 0–50,000 Ωm according to the manufacturer. The rock resistivity was also logged using the Century 9033 tool. However, this tool may not be suitable for quantitative logging in granitic rock and the results are not used in this report.

3.2 Groundwater electrical conductivity measurements

The EC (electrical conductivity) of the borehole fluid in KFM05A /3/ and KFM06A /4/ was logged using the POSIVA difference flow meter. The tool is shown in Figure 3-1.

When logging the EC of the borehole fluid, the lower rubber disks of the tool are not used. During the measurements, a drawdown can either be applied or not. Measurements were carried out before and after extensive pumping in borehole KFM06A. In KFM05A, borehole fluid EC measurements were only carried out after extensive pumping.

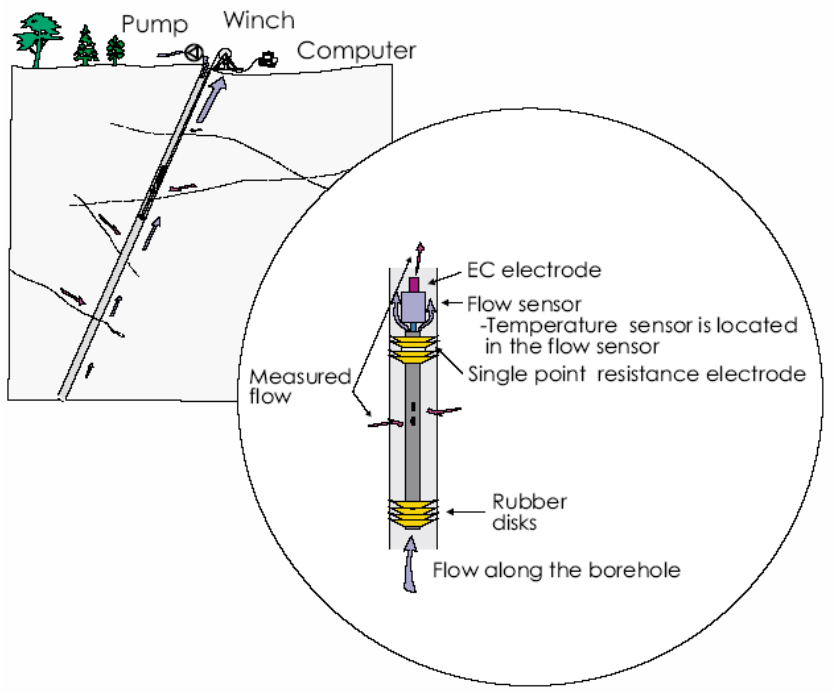

Figure 3-1. *Schematics of the POSIVA difference flow meter (image taken from /3/).*

When using both the upper and the lower rubber disks, a section around a specific fracture can be packed off. By applying a drawdown at the surface, groundwater can thus be extracted from specific fractures. This is done in fracture specific EC measurements. By also measuring the groundwater flow out of the fracture, it is calculated how long time it will take to fill up the packed off borehole section three times. During this time the EC is measured and a transient EC curve is obtained. After this time it is assumed that the measured EC is representative for the groundwater flowing out of the fracture. The measurements may be disturbed by leakage of borehole fluid into the packed off section and development of gas from species dissolved in the groundwater. Interpretations of transient EC curves are discussed in /5/. The quantitative measuring range of the EC electrode of the POSIVA difference flow meter is 0.02–11 S/m.

The EC, among other entities, of the groundwater coming from fractures in larger borehole sections is measured as a part of the hydrochemical characterisation. A section is packed off and by using a drawdown, groundwater is extracted from fractures within the section and brought to the surface for chemical analysis. Hydrochemical characterisations of KFM05A /6/ and KFM06A /7/ were performed in two different campaigns.

3.3 Difference flow loggings

By using the POSIVA difference flow meter, water-conducting fractures can be located. The tool, shown in Figure 3-1, has a flow sensor and the flow from fractures in packed off sections can be measured. When performing these measurements, both the upper and the lower rubber disks are used. Measurements can be carried out both with and without applying a drawdown. The quantitative measuring range of the flow sensor is 0.1–5,000 ml/min.

Difference flow loggings were performed in two different campaigns in KFM05A /3/ and KFM06A /4/.

3.4 Boremap loggings

The drill cores of KFM05A /8/ and KFM06A /9/ were logged together with a simultaneous study of video images of the borehole wall. This is called Boremap logging.

In the core log, fractures parting the core are recorded. Fractures parting the core that have not been induced during the drilling or core handling are called broken fractures. To decide if a fracture actually was open or sealed in the rock volume (i.e. in-situ), SKB has developed a confidence classification expressed at three levels, “possible”, “probable” and “certain”, based on the weathering and fit of the fracture surfaces /8/. However, there is a strong uncertainty associated with determining whether broken fractures were open or not before drilling /10/. For this reason, it was decided to treat all broken fractures as potentially open in-situ in this present report.

In the Boremap logging, parts of the core that are crushed or lost are also recorded, as well as the spatial distribution of different rock types.

4 Execution

4.1 Theory

4.1.1 The formation factor

The theory applied for obtaining formation factors by electrical methods is described in /11/. The formation factor is the ratio between the diffusivity of the rock matrix to that of free pore water. If the species diffusing through the porous system is much smaller than the characteristic length of the pores and no interactions occur between the mineral surfaces and the species, the formation factor is only a geometrical factor that is defined by the transport porosity, the tortuosity and the constrictivity of the porous system:

$$F_f = \frac{D_e}{D_w} = \varepsilon_t \frac{\delta}{\tau^2} \qquad 4\text{-}1$$

where Ff (–) is the formation factor, De (m^2/s) is the effective diffusivity of the rock, Dw (m^2/s) is the diffusivity in the free pore water, ε_t (–) is the transport porosity, τ (–) is the tortuosity, and δ (–) is the constrictivity. When obtaining the formation factor with electrical methods, the Einstein relation between diffusivity and ionic mobility is used:

$$D = \frac{\mu RT}{zF} \qquad 4\text{-}2$$

where D (m^2/s) is the diffusivity, μ ($m^2/V \times s$) is the ionic mobility, z (–) the charge number and R (J/mol×K), T (K) and F (C/mol), are the gas constant, temperature, and Faraday constant respectively. From the Einstein relation it is easy to show that the formation factor also is given by the ratio of the pore water resistivity to the resistivity of the saturated rock /12/:

$$F_f = \frac{\rho_w}{\rho_r} \qquad 4\text{-}3$$

where ρ_w (Ωm) is the pore water resistivity and ρ_r (Ωm) is the rock resistivity. The resistivity of the saturated rock can easily be obtained by standard geophysical methods.

At present it is not feasible to extract pore water from the rock matrix in-situ. Therefore, it is assumed that the pore water is in equilibrium with the free water surrounding the rock, and measurements are performed on this free water. The validity of this assumption has to be discussed for every specific site. In a new line of experiments, species in the pore water in drill core samples brought to the laboratory are leached. This was done in KFM06A /13/ and the results from these measurements are used when validating the assumed electrical conductivity profile of the groundwater and pore water.

The resistivity is the reciprocal to electrical conductivity. Traditionally the EC (electrical conductivity) is used when measuring on water and resistivity is used when measuring on rock.

4.1.2 Surface conductivity

In intrusive igneous rock the mineral surfaces are normally negatively charged. As the negative charge often is greater than what can be balanced by cations specifically adsorbed on the mineral surfaces, an electrical double layer with an excess of mobile cations will form at the pore wall. If a potential gradient is placed over the rock, the excess cations in the electrical double layer will move. This process is called surface conduction and this additional conduction may have to be accounted for when obtaining the formation factor of rock saturated with a pore water of low ionic strength. If the EC of the pore water is around 0.5 S/m or above, errors associated with surface conduction are deemed to be acceptable. This criterion is based on laboratory work by /12/ and /14/. The effect of the surface conduction on rock with formation factors below 1×10^{-5} was not investigated in these works. In this report, surface conduction has not been accounted for, as only the groundwater in the upper 100 or 200 m of the boreholes has a low ionic strength and as more knowledge is needed on surface conduction before performing corrections.

4.1.3 Artefacts

Comparative studies have been performed on a large number of 1–2 cm long samples from Äspö in Sweden /14/. Formation factors obtained with an electrical resistivity method using alternating current were compared to those obtained by a traditional through diffusion method, using Uranine as the tracer. The results show that formation factors obtained by the electrical resistivity measurements are a factor of about 2 times larger that those obtained by through diffusion measurements. A similar effect was found on granitic samples up to 12 cm long, using iodide in tracer experiments /15/. The deviation of a factor 2 between the methods may be explained by anion exclusion of the anionic tracers. Previously performed work suggests that the Nernst-Einstein equation between the diffusivity and electrical conductivity is generally applicable in granitic rock and that no artefacts give rise to major errors. It is uncertain, however, to what extent anion exclusion is related to the degree of compression of the porous system in-situ due to the overburden.

4.1.4 Fractures in-situ

In-situ rock resistivity measurements are highly disturbed by free water in open fractures. The current sent out from the downhole tool in front of an open fracture will be propagated both into the porous system of the rock matrix and in the free water in the open fracture. Due to the low formation factor of the rock matrix, current may be preferentially propagated into a fracture intersecting the borehole if its aperture is on the order of 10^{-5} m or more.

There could be some confusion concerning the terminology of fractures. In order to avoid confusion, an organization sketch of different types of fractures is shown in Figure 4-1. The subgroups of fractures that interfere with the rock resistivity measurements are marked with grey.

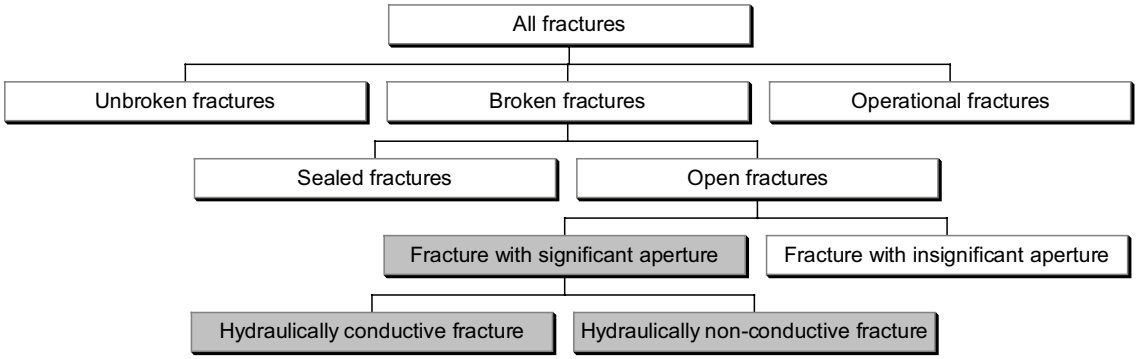

Figure 4-1. *Organization sketch of different types of fractures in-situ.*

The information concerning different types of fractures in-situ is obtained from the interpretation of the Boremap logging and in the hydraulic flow logging. A fracture intersecting the borehole is most likely to part the drill core. In the core log, fractures that part the core are either broken or operational (drill-induced). Unbroken fractures, which do not part the core, are sealed or only partly open. Laboratory results suggest that sealed fractures generally have no major interference on rock resistivity measurements. The water-filled void in partly open fractures can be included in the porosity of the rock matrix.

Broken fractures are either interpreted as open or sealed. Open fractures may have a significant or insignificant aperture. Insignificant aperture refers to an aperture so small that the amount of water held by the fracture is comparable with that held in the adjacent porous system. In this case the "adjacent porous system" is the porous system of the rock matrix existing within the first few centimetres from the fracture.

If the fracture has a significant aperture, it holds enough water to interfere with the rock resistivity measurements. Fractures with a significant aperture may be hydraulically conductive or non-conductive, depending on how they are connected to the fracture network.

Due to uncertainties in the interpretation of the core logging, all broken fractures are assumed to potentially have a significant aperture.

4.1.5 Rock matrix and fractured rock formation factor

In this report the rock resistivity is used to obtain formation factors of the rock surrounding the borehole. The obtained formation factors may later be used in models for radionuclide transport in fractured crystalline rock. Different conceptual approaches may be used in the models. Therefore this report aims to deliver formation factors that are defined in two different ways. The first is the "rock matrix formation factor", denoted by F_f^{rm} (–). This formation factor is representative for the solid rock matrix, as the traditional formation factor. The other one is the "fractured rock formation factor", denoted by F_f^{fr} (–), which represents the diffusive properties of a larger rock mass, where fractures and voids holding stagnant water is included in the porous system of the rock matrix. Further information on the definition of the two formation factors could be found in /5/.

The rock matrix formation factor is obtained from rock matrix resistivity data. When obtaining the rock matrix resistivity log from the in-situ measurements, all resistivity data that may have been affected by open fractures have to be sorted out. With present methods one cannot with certainty separate open fractures with a significant aperture from open fractures with an insignificant aperture in the interpretation of the core logging. It should be mentioned that there is an attempt to assess the fracture aperture in the interpretation of the core logging. However, this is done on a millimetre scale. Fractures may be significant even if they only have apertures some tens of micrometres.

By investigating the rock resistivity log at a fracture, one could draw conclusions concerning the fracture aperture. However, for formation factor logging by electrical methods this is not an independent method and cannot be used. Therefore, all broken fractures have to be considered as potentially open and all resistivities obtained close to a broken fracture detected in the core logging are sorted out. By examining the resistivity logs obtained by the Century 9072 tool, it has been found that resistivity values obtained within 0.5 m from a broken fracture generally should be sorted out. This distance includes a safety margin of 0.1–0.2 m.

The fractured rock formation factor is obtained from fractured rock resistivity data. When obtaining the fractured rock resistivity log from the in-situ measurements, all resistivity data that may have been affected by free water in hydraulically conductive fractures, detected in the in-situ flow logging, have to be sorted out. By examining the resistivity logs obtained by the Century 9072 tool, it has been found that resistivity values obtained within 0.5 m from a hydraulically conductive fracture generally should be sorted out. This distance includes a safety margin of 0.1–0.2 m.

4.2 Rock resistivity measurements in-situ

4.2.1 Rock resistivity log KFM05A

The rock resistivity of KFM05A was logged on the date 2004-05-20 (activity id 13029597) /1/. The in-situ rock resistivity was obtained using the focused rock resistivity tool Century 9072. In-situ rock resistivites, used in this present report, were obtained between the borehole lengths 112–1,000 m. In order to obtain an exact depth calibration, the track marks made in the borehole were used. According to /1/ an exact depth calibration was not obtained. The following deviations in the calibration with depth are reported.

The deviation is fairly linear with the borehole length. The borehole length reported in /1/ was corrected between 120–1,000 m by subtracting the deviation obtained by the linear equation shown in Figure 4-2.

In Figure 4-2 the borehole length on the x-axis is according to the reference marks. In the equation in Figure 4-2, the "Borehole length" is the uncorrected borehole length. No correction in reported borehole length was made between 0–120 m.

4.2.2 Rock matrix resistivity log KFM05A

After adjusting the borehole length of the in-situ rock resistivity log, all resistivity data obtained within 0.5 m from a broken fracture detected in the core log were sorted out. In the core log (activity id 13060685), a total of 1,091 broken fractures are recorded between 102.3–999.5 m.

Table 4-1. Deviation in borehole lengths. Data from /1/.

Reference mark (m)	120	152	199	252	300	352	402	450	606
Deviation (m)	0	0.02	0.03	0.14	0.19	0.25	0.36	0.37	0.72
Reference mark (m)	750	800	850	900					
Deviation (m)	0.98	0.97	1.04	1.09					

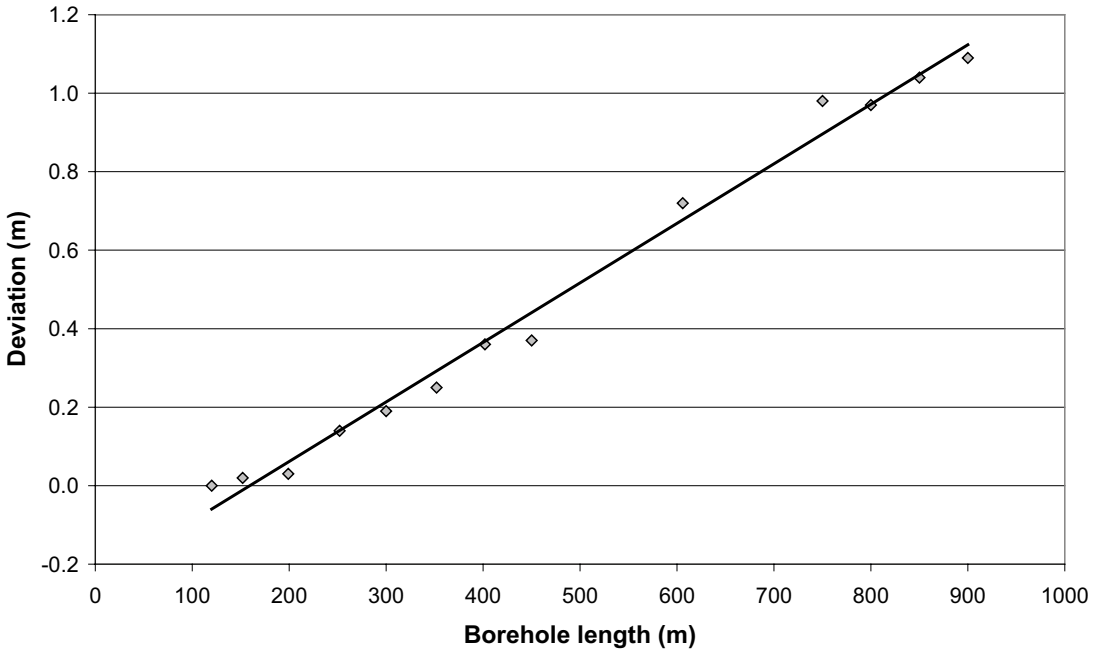

Figure 4-2. *Deviations in borehole length in KFM05A.*

Three crush zones and three zones where the core has been lost are recorded. A total of 0.74 m of the core was crushed or lost. Broken fractures can potentially intersect the borehole in zones where the core is crushed or lost. Therefore, a broken fracture was assumed every decimetre in these zones. The locations of broken fractures in KFM05A are shown in Appendix B1. A total of 4,227 rock matrix resistivities were obtained between 112–1,000 m. 3,995 (95%) of the rock matrix resistivities were within the quantitative measuring range of the Century 9072 tool. The rock matrix resistivity log between 112–1,000 m is shown in Appendix B1.

Figure 4-3 shows the distribution of the rock matrix resistivities obtained between 112–1,000 m in KFM05A. The histogram ranges from 0–100,000 Ωm and is divided into sections of 5,000 Ωm.

4.2.3 Fractured rock resistivity log KFM05A

After adjusting the borehole length of the in-situ rock resistivity log, all resistivity data obtained within 0.5 m from a hydraulically conductive fracture, detected in the difference flow logging /3/, were sorted out. For the difference flow log, no correction in the reported borehole length was needed. A total of 27 hydraulically conductive fractures were detected in KFM05A. The locations of hydraulically conductive fractures in KFM05A are shown in Appendix B1. A total of 8,685 fractured rock resistivities were obtained between 112–1,000 m. 8,042 (93%) of the fractured rock resistivities were within the quantitative measuring range of the Century 9072 tool. The fractured rock resistivity log between 112–1,000 m is shown in Appendix B1.

Figure 4-4 shows a histogram of the fractured rock resistivities obtained between 112–1,000 m in KFM05A. The histogram ranges from 0–100,000 Ωm and is divided into sections of 5,000 Ωm.

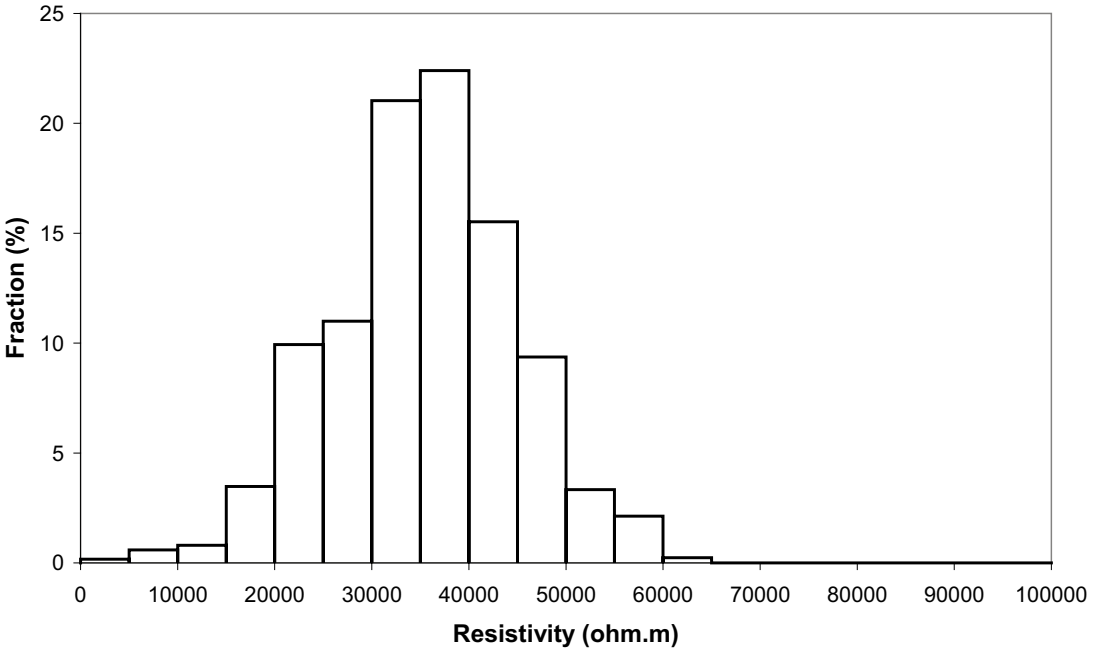

Figure 4-3. *Distribution of rock matrix resistivities in KFM05A.*

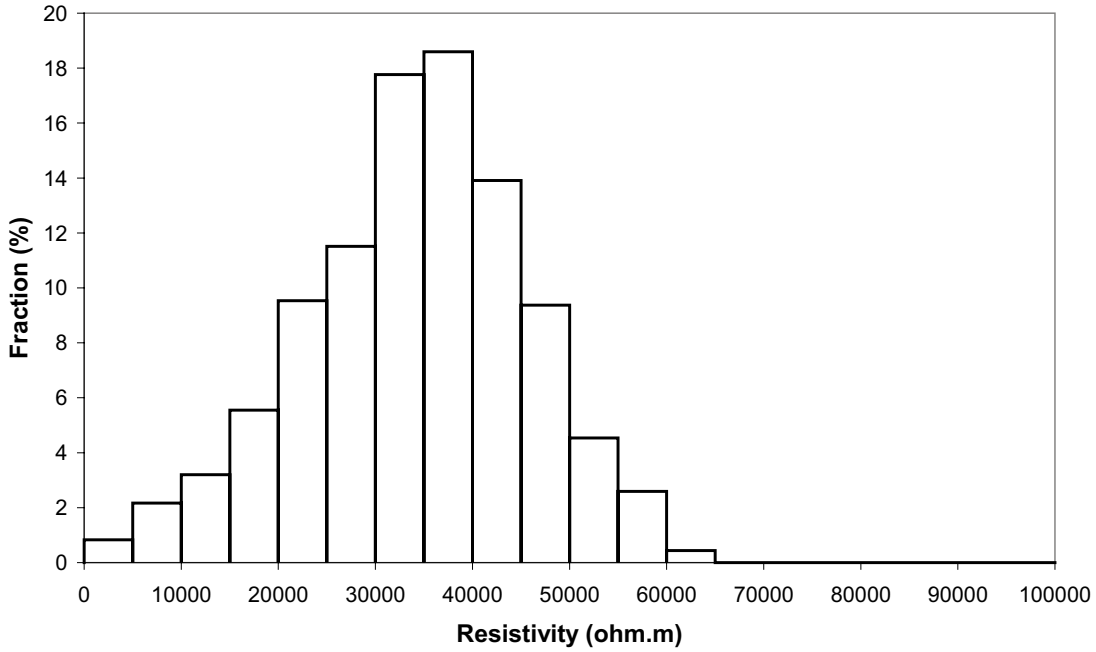

Figure 4-4. *Histogram of fractured rock resistivities in KFM05A.*

4.2.4 Rock resistivity KFM06A

The rock resistivity of KFM06A was logged on the date 2004-11-04 (activity id 13101664) /2/. The in-situ rock resistivity was obtained using the focused Century 9072 tool. In-situ rock resistivites, used in this present report, were obtained between the borehole lengths 104–996 m. In order to obtain an exact depth calibration, the track marks made in the borehole were used. According to /2/ an accurate depth calibration was obtained.

4.2.5 Rock matrix resistivity log KFM06A

All resistivity data obtained within 0.5 m from a broken fracture, detected in the core log, were sorted out. In the core log (activity id 13074960), a total of 1,403 broken fractures are recorded between 102.2–997.4 m. In addition, four crush zones but no zones where the core is lost are recorded. A total of 0.67 m of the core is crushed. Broken fractures can potentially intersect the borehole in zones where the core is crushed or lost. Therefore, a broken fracture was assumed every decimetre in these zones. The locations of broken fractures in KFM06A are shown in Appendix B2. A total of 2,880 rock matrix resistivities were obtained between 104–996 m. 2,670 (93%) of the rock matrix resistivities were within the quantitative measuring range of the Century 9072 tool. The rock matrix resistivity log between 104–996 m is shown in Appendix B2.

Figure 4-5 shows a histogram of the rock matrix resistivities obtained between 104–996 m in KFM06A. The histogram ranges from 0–100,000 Ωm and is divided into sections of 5,000 Ωm.

4.2.6 Fractured rock resistivity log KFM06A

All resistivity data obtained within 0.5 m from a hydraulically conductive fracture, detected in the difference flow logging /4/, were sorted out. For the difference flow log, no correction in the reported borehole length was needed. A total of 99 hydraulically conductive fractures were detected in KFM06A. The locations of hydraulically conductive fractures in KFM06A are shown in Appendix B2. A total of 8,091 fractured rock resistivities were obtained between 104–996 m. 7,675 (95%) of the fractured rock resistivities were within the quantitative measuring range of the Century 9072 tool. The fractured rock resistivity log between 104–996 m is shown in Appendix B2.

Figure 4-6 shows a histogram of the fractured rock resistivities obtained between 104–996 m in KFM06A. The histogram ranges from 0–100,000 Ωm and is divided into sections of 5,000 Ωm.

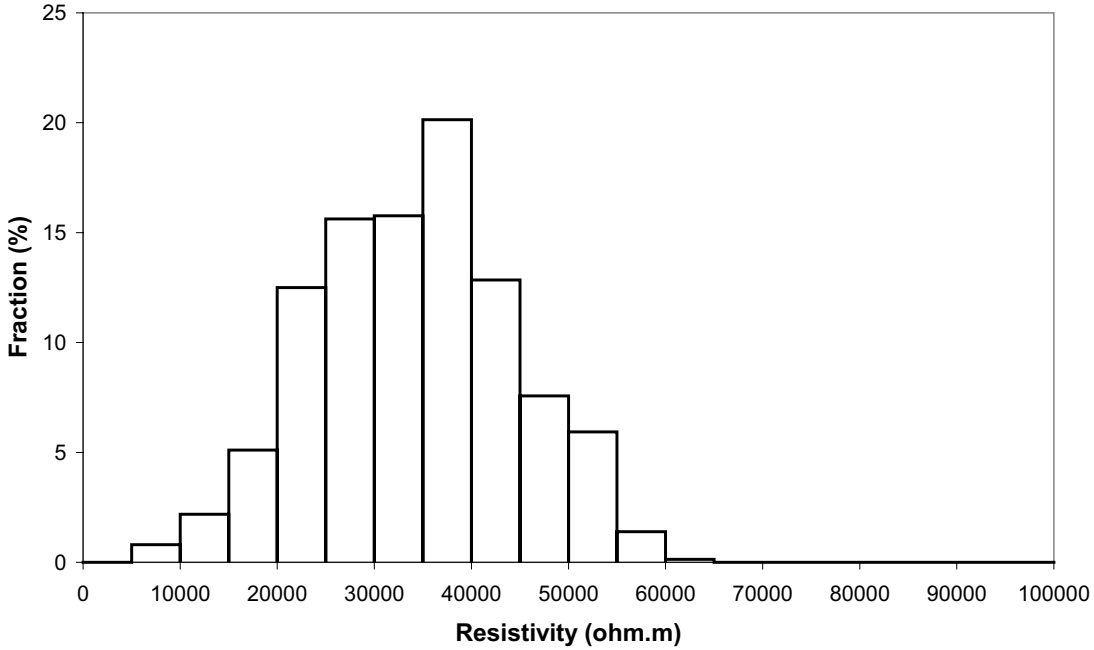

Figure 4-5. *Histogram of rock matrix resistivities in KFM06A.*

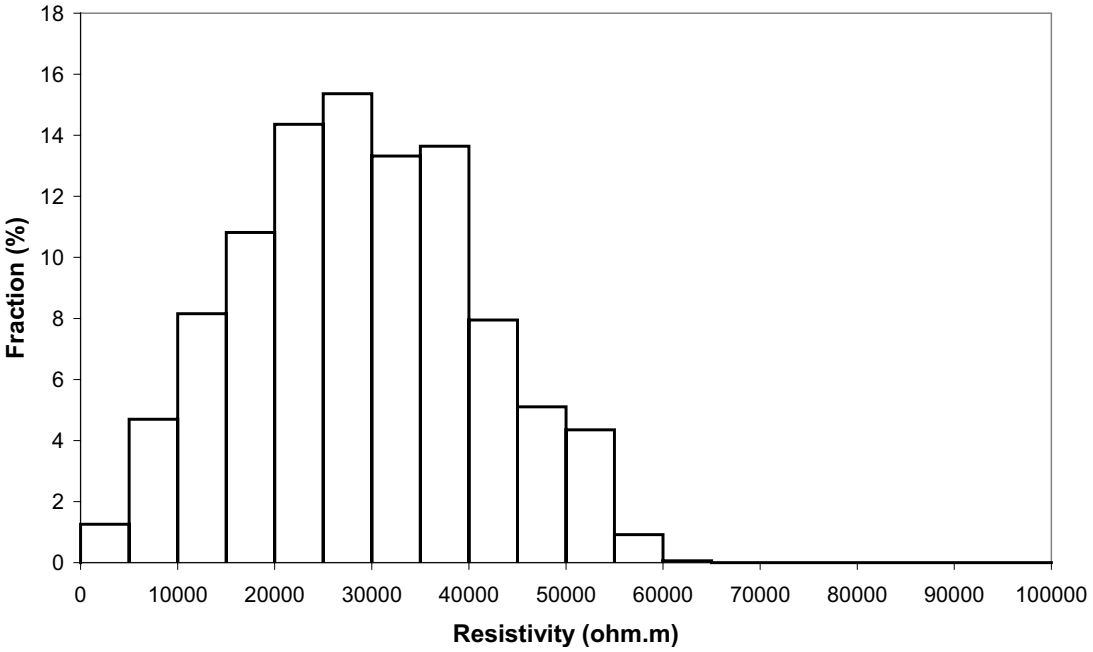

Figure 4-6. *Histogram of fractured rock resistivities in KFM06A.*

4.3 Groundwater EC measurements in-situ

4.3.1 General comments

In background reports concerning the EC of the groundwater, some data have been corrected for temperature, so that they correspond to data at 25°C. Other EC data are uncorrected. Data that correspond to the temperature in-situ should be used in in-situ evaluations. Even though these corrections are small in comparison to the natural variation of the formation factor, measures have been taken to use data that correspond to the in-situ temperature. In some instances, EC data corrected to 25°C have been corrected once more so that they correspond to the in-situ temperature.

4.3.2 EC measurements in KFM05A

The EC of the borehole fluid in KFM05A was measured on the date 2004-05-31 after performing extensive pumping /3/. For this reason, water from the lower part of the borehole had been brought up to shallower parts and little information can be extracted from the borehole fluid EC. What can be suggested is that there appears to be an anomaly at about 120 m. Above this borehole length there is a natural flow into the borehole and below this borehole length there is a natural flow out from the borehole. Furthermore, at some depth in the lower part of the borehole, the groundwater EC is at least as high as 1.0 S/m.

The EC of groundwater extracted from a number of specific fractures between 108–265 m was measured by using the POSIVA difference flow meter /3/. The measurements were carried out between the dates 2004-05-30 and 2004-06-02. The resulting fracture specific ECs are shown in Table 4-2. From the transient fracture specific EC curves, one can suspect that borehole fluid disturbed the measurement at the fracture at 108.9 m. Therefore, the ECs at this depth are disregarded in this report. After studying the transient fracture specific EC curves obtained at the other fractures, the EC values shown in Table 4-2 are judged as reasonable.

The EC of groundwater extracted from a packed off section between 712.6 and 722.0 m in KFM05A was measured in the hydrochemical characterisation /6/. The hydrochemical characterisation was started on the date 2004-09-18 and carried out for about one month. The resulting fracture specific EC is shown in Table 4-2.

4.3.3 EC measurements in KFM06A

The EC of the borehole fluid in KFM06A was measured before and after extensive pumping in a difference flow logging campaign on the dates 2004-10-13 and 2004-10-20, respectively /4/.

The EC of groundwater extracted from a number of specific fractures between 125–744 m was measured in a campaign using the POSIVA difference flow meter /4/. The measurements were carried out between the dates 2004-10-19 and 2004-10-20. The resulting fracture specific ECs are shown in Table 4-3. After inspecting the transient fracture specific EC curves, all values are judged as reasonable.

The EC of groundwater extracted from two packed off sections of KFM06A was measured in the hydrochemical characterisation /7/. The hydrochemical characterisation was carried out between the dates 2004-11-24 and 2002-03-22. The resulting fracture specific ECs are shown in Table 4-3.

Table 4-2. Fracture specific ECs, KFM05A.

Measurement	Borehole section (m)	Location of ractures (m)	EC in-situ (S/m)	EC 25°C(S/m)
Difference flow	108.4–109.4	108.9	(0.93)	(1.41)
Difference flow	108.7–109.7	108.9	(0.83)	(1.26)
Difference flow	116.2–117.2	116.5	1.04	1.56
Difference flow	123.8–124.8	124.1, 124.4	1.02	1.54
Difference flow	175.0–176.0	175.6	0.97	1.44
Difference flow	264.0–265.0	264.4	0.97	1.41
Hydrochemical characterisation	712.6–722.0	720	1.04*	1.38

*Obtained by using temperature correction based on /3/ at that depth.

Table 4-3. Fracture specific ECs, KFM06A.

Measurement	Borehole section (m)	Location of fractures (m)	EC in-situ (S/m)	EC 25°C (S/m)
Difference flow	125.29–126.29	126.0	0.78	1.18
Difference flow	127.99–128.99	128.5, 128.9	0.91	1.38
Difference flow	128.80–129.80	128.9, 129.4	0.97	1.46
Difference flow	129.60–130.60	130.3	0.97	1.46
Difference flow	131.00–132.00	131.7, 132.0	0.96	1.44
Difference flow	134.71–135.71	135.0, 135.4	0.95	1.43
Difference flow	176.77–177.77	177.4	1.02	1.51
Difference flow	180.47–181.47	181.0, 181.2	1.00	1.49
Difference flow	217.49–218.49	218.2	0.99	1.46
Difference flow	237.25–238.25	238.0	1.01	1.48
Difference flow	267.89–268.89	268.6	0.98	1.43
Difference flow	268.69–269.69	269.3	0.99	1.45
Difference flow	356.10–357.10	356.6	0.81	1.17
Difference flow	742.79–743.79	743.3	1.03	1.36
Hydrochemical characterisation	353.5–360.6	354.2, 356.6	0.93*	1.34
Hydrochemical characterisation	768.0–775.1	770.6, 770.8	1.49*	1.95

*Obtained by using temperature correction based on /4/ at that depth.

The borehole fluid EC log obtained before the fracture specific EC measurements in KFM06A is shown in Figure 4-7, together with the fractures specific ECs shown in Table 4-3. If there are more than one fracture in a packed off section, the mean value of the borehole lengths of the fractures is used.

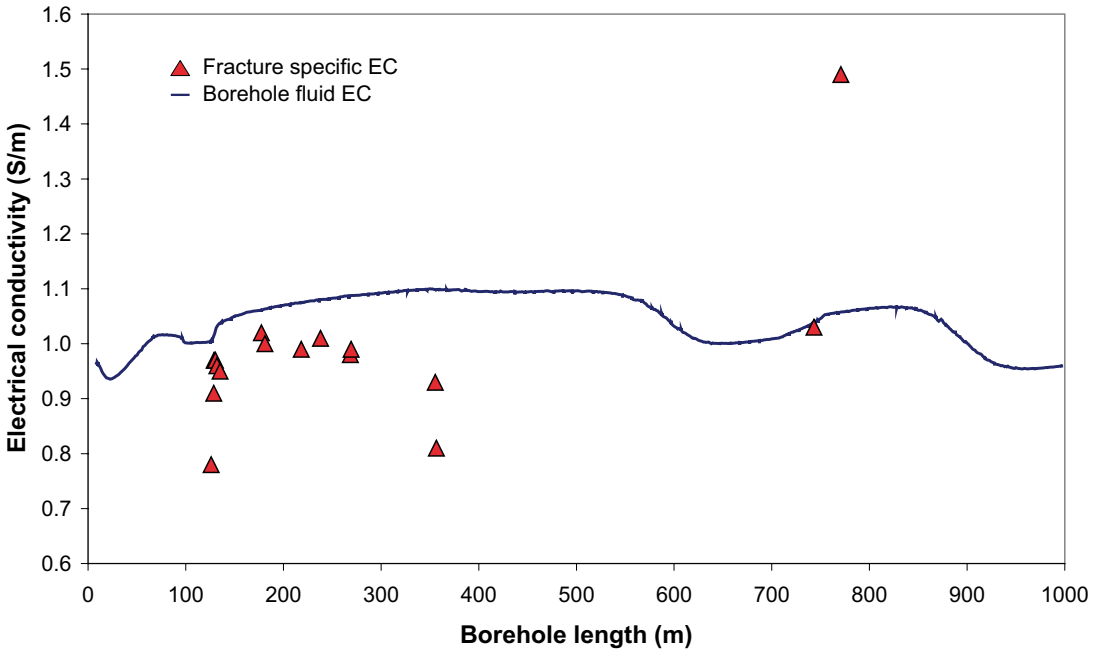

Figure 4-7. Groundwater EC in KFM06A.

4.3.4 EC measurements in KFM01A–KFM06A

In KFM05A and KFM06A, fracture specific groundwater ECs were obtained down to a borehole length of 720 m and 770 m, respectively. In order to obtain groundwater EC profiles in the boreholes, especially in the lowest parts of the boreholes, fracture specific ECs from difference flow measurements and hydrochemical characterisations in the boreholes KFM01A-KMF06A were used. As the boreholes have different inclinations, this was corrected for and the x-axis in Figure 4-8 represents the vertical borehole depth. Different altitudes of the drilling sites were not corrected for. In Figure 4-8 the EC values should correspond to the in-situ temperature. The values are tabulated in Appendix D.

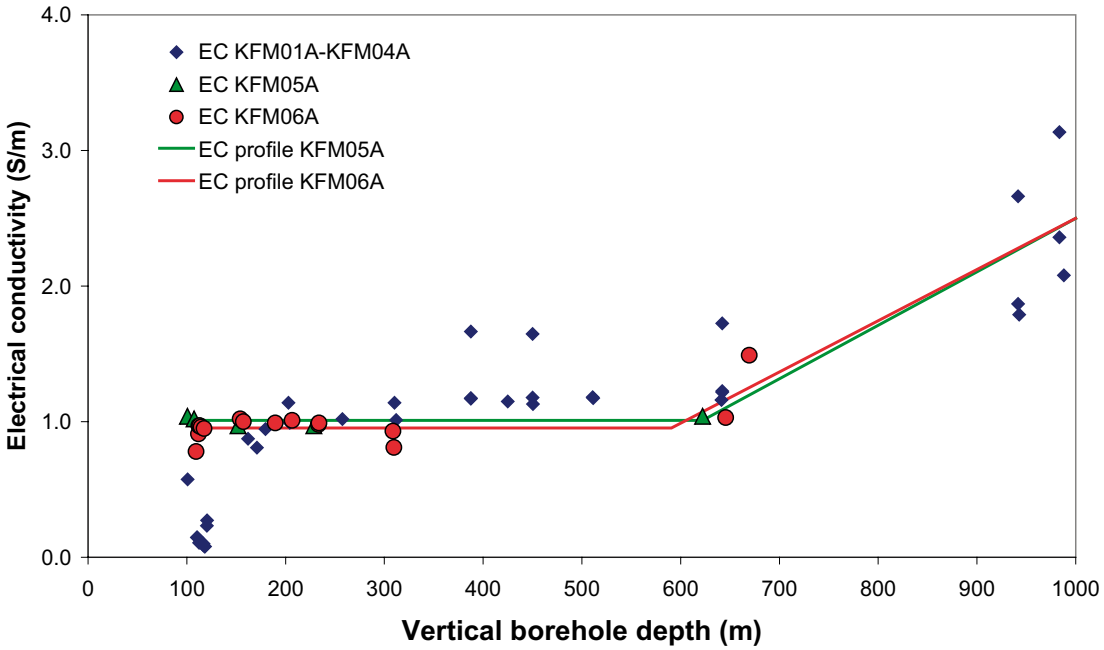

Figure 4-8. Groundwater EC in KFM01A–KFM06A.

The green and red lines shown in Figure 4-8 are the obtained EC profiles for KFM05A and KFM06A, respectively. Obtaining such profiles is a somewhat subjective operation, due to lack of data. However, the variations in the EC of the groundwater are generally small in comparison to the variation in formation factor. The exception is the transition from fresh-meteoric waters to brackish-marine waters in the upper 200 m of the bedrock /16/. This transition appears to have occurred in the upper 100 m in both boreholes. It is recommended not to extrapolate the obtained EC profiles to borehole lengths smaller that 116 m and 126 m for KFM05A and KFM06A, respectively.

The equations for the EC-profiles shown in Figure 4-8 are the following:

KFM05A: borehole length 116–720 m,

$$EC\ (S/m) = 1.01 \qquad 4\text{-}4$$

KFM05A: borehole length 720–1,001 m,

$$EC\ (S/m) = 3.41\times10^{-3}\times\text{borehole length (m)} - 1.44 \qquad 4\text{-}5$$

KFM06A: borehole length 126–680 m,

$$EC\ (S/m) = 0.95 \qquad 4\text{-}6$$

KFM06A: borehole length 680–1,003 m,

$$EC\ (S/m) = 3.28\times10^{-3}\times\text{borehole length (m)} - 1.28 \qquad 4\text{-}7$$

4.3.5 Electrical conductivity of the pore water

In KFM05A, on average 1.6 broken fractures per metre part the drill core. From the rock resistivity log one can see that a substantial fraction of the broken fractures are open with a significant aperture. By visual inspection of the rock resistivity logs, shown in Appendix B1, one can see that the typical block of solid rock between open fractures with significant apertures is a few metres wide or less. In some cases the block size is larger. No extensive difference in fracture frequency can be seen between the upper and lower part of the borehole. According to the measurements with the difference flow meter /3/, the upper 180 m of the borehole feature numerous hydraulically conductive fractures. Below 180 m, only 3 hydraulically conductive fractures were found and below 720 m, none. As much of the borehole features so few hydraulically conductive fractures, the suggested EC profile is somewhat speculative.

Also in KFM06A, on average 1.6 broken fractures per metre part the drill core. From the rock resistivity log one can see that a substantial fraction of the broken fractures are open with a significant aperture. By visual inspection of the rock resistivity logs, shown in Appendix B1, one can see that the typical block of solid rock between open fractures with significant apertures is a few metres wide or less. In a few cases the block size is larger. No extensive difference in fracture frequency can be seen between the upper and lower part of the borehole. According to the measurements with the difference flow meter /4/, the upper part 360 m of the borehole intersect numerous hydraulically conductive fractures. Below 360 m, only 8 hydraulically conductive fractures were found and below 770 m, none. As the lower part of the borehole like in KFM05A features so few hydraulically conductive fractures, the suggested EC profile is somewhat speculative.

In a new line of experiments, species in the matrix pore water in drill core samples brought to the laboratory are leached. This was done in KFM06A /13/ and the results from these measurements are used when validating the assumed electrical conductivity profile of the groundwater and pore water. Figure 4-9 shows the obtained chloride concentration of the matrix pore water /13/.

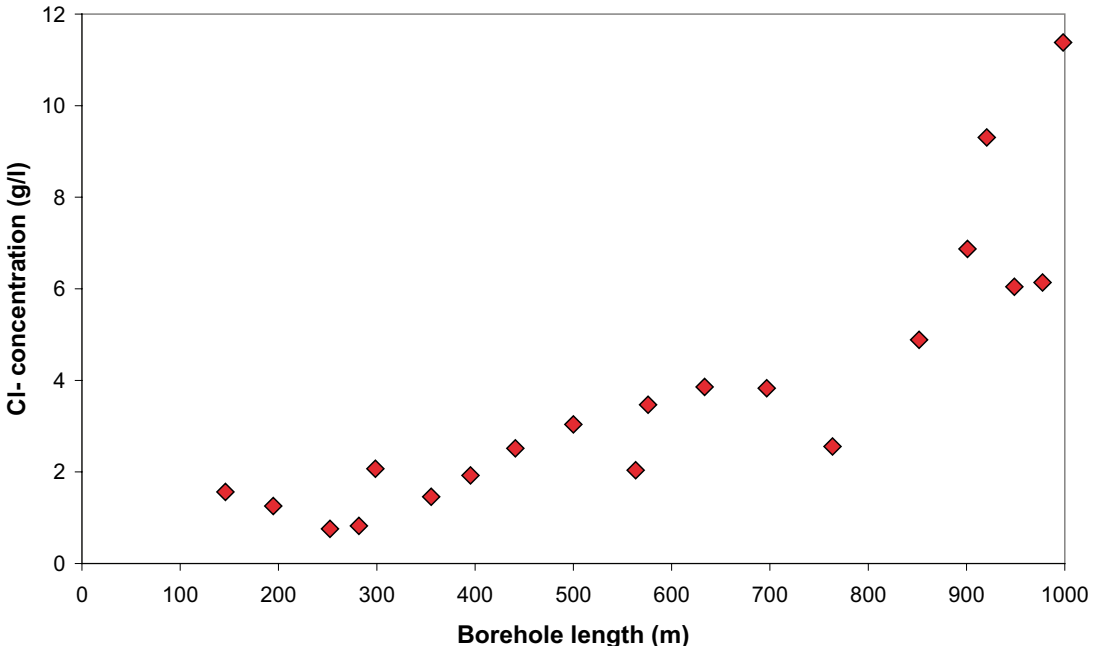

Figure 4-9. *Chloride concentration of matrix pore water obtained on core samples /13/.*

In order to compare the data in Figure 4-9 with those in Figure 4-8, the chloride concentrations need to be converted to ECs. This was done, by somewhat crude means, by using a linear relation between the entities. The relation was obtained by using the least square method on data from the hydrochemical characterisation of KFM06A /7/, where both EC and chloride concentration were obtained on groundwater samples from a few fractures. It should be noted that the more non-saline the water is, the less reliable the linear relation becomes. The temperature correction is based on data from /4/. Figure 4-10 shows the obtained matrix pore water EC, as well as the assumed EC profile (green line) that is also shown in Figure 4-8.

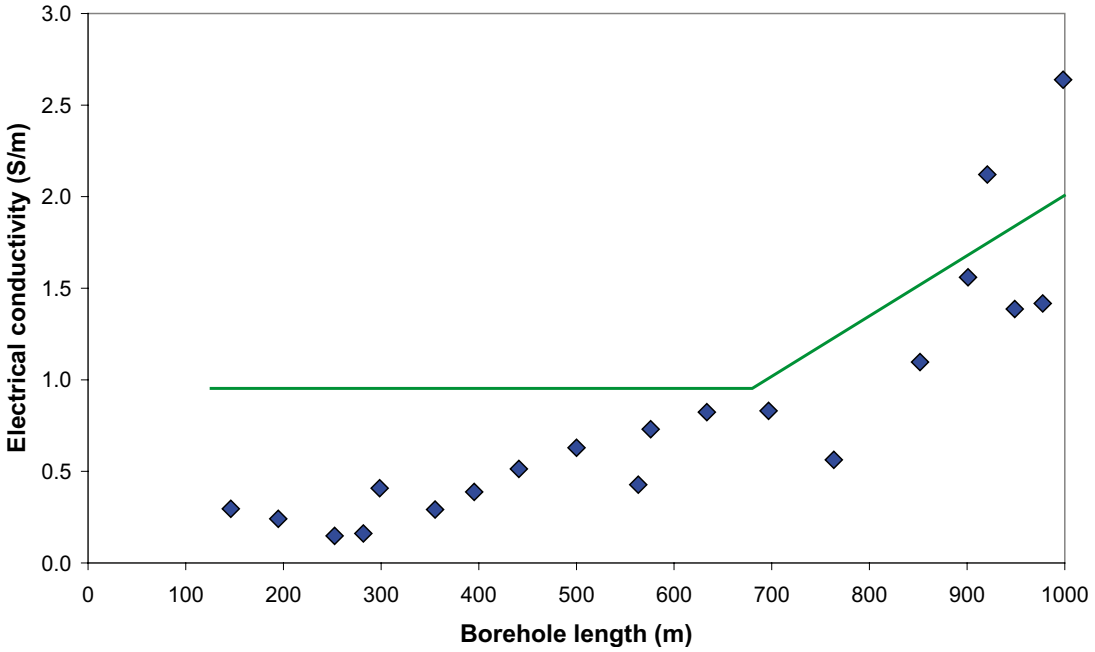

Figure 4-10. *Approximate EC of matrix pore water obtained on core samples /13/.*

In the lower part of the borehole, the assumed EC profile corresponds well to the ECs of the matrix pore water obtained on core samples /13/. In the first few hundred metres, the deviation is about a factor of 3 to 4. Compared to the natural variation of the formation factor, the deviation is significant but still small. It should be noted that the chloride concentrations, obtained when leaching matrix pore water from core samples, also are associated with errors.

The typical spacing of solid rock blocks between open fractures is for both boreholes a few metres. Even the centre of such a block would be fairly well equilibrated with non-sorbing solutes in a 1,000 years perspective. Figure 4-10 substantiates this conclusion. Even though the profiles do not correspond perfectly, they give the same picture of EC profile. Furthermore it is interesting to note that no chloride concentration obtained on the core samples in /13/ deviates significantly from the general trend, i.e. suggesting a non-equilibrated (isolated) block of rock. In all fairness it should be pointed out that the results do not suggest the opposite either.

It is judged that the suggested EC profiles for KFM05A and KFM06A are reasonable.

4.4 Formation factor measurements in the laboratory

The laboratory work was performed by Geovista AB. Formation factors were obtained on 23 rock samples taken from the drill core of KFM05A /17/.The sample length was, in general, 3 cm. The obtained formation factors are tabulated in Appendix A1. Formation factors have not been obtained in the laboratory for borehole KFM06A.

4.5 Nonconformities

The work was carried out in accordance with the activity plan and the method description without nonconformities. However, the limited quantitative measuring range of the in-situ rock resistivity tool may give overestimations of formation factors in the lower formation factor range.

5 Results

5.1 Laboratory formation factor

The formation factors obtained in the laboratory are tabulated in Appendix A1 for KFM05A.

The 23 laboratory formation factors obtained in KFM05A were treated statistically. By using the normal-score method, as described in /18/, to determine the likelihood that a set of data is normally distributed, the mean value and standard deviation of the logarithm ($\log_{10}$) of the formation factors could be determined. Figure 5-1 shows the distribution of the laboratory formation factors obtained in KFM05A.

As can be seen in Figure 5-1, the obtained formation factors range over two orders of magnitude and deviates slightly from the log-normal distribution. However, it should be kept in mind that only a few data points were used. The mean value and standard deviation of the distribution in Figure 5-1 are shown in Table 5-1. The laboratory formation factor logs of KFM05A are shown in Appendix C1, as compared to the in-situ formation factor logs.

Table 5-1. Distribution parameters and arithmetic mean value of the formation factor, KFM05A.

Formation factor	Number of data points	Mean $\log_{10}(F_f)$	Standard deviation $\log_{10}(F_f)$	Arithmetic mean F_f
Laboratory F_f	23	–3.77	0.293	2.05×10^{-4}
In-situ Rock matrix F_f	4,220	–4.59	0.170	2.82×10^{-5}
In-situ Fractured rock F_f	8,760	–4.55	0.206	3.32×10^{-5}

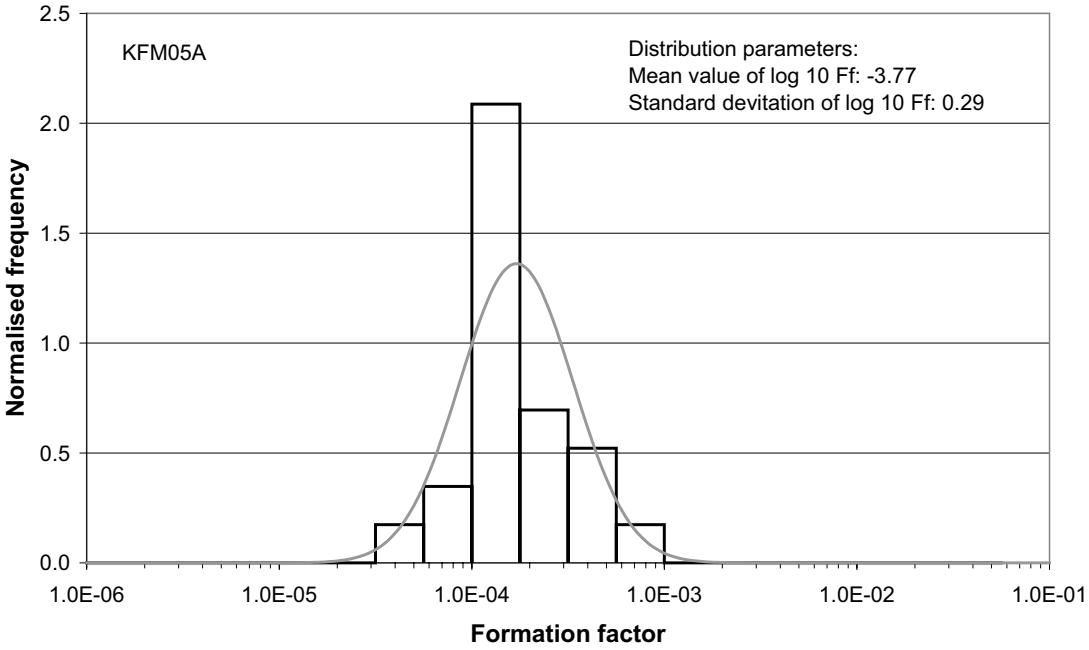

Figure 5-1. *Distribution of laboratory formation factors in KFM05A.*

5.2 In-situ rock matrix formation factor

Figure 5-2 shows the distributions of the rock matrix formation factors obtained in-situ in KFM05A and KFM06A.

The rock matrix formation factors are log-normally distributed. For KFM05A, there is a slight tailing between 10^{-4} and 10^{-3} that may not represent the rock matrix formation factor. As can be seen at some borehole lengths in Appendix B1, e.g. at 760 m, there is a slight deviation between the borehole lengths in the rock resistivity log and drill core log. The result is that some rock resistivities measured at fractures are sorted as rock matrix resistivities. These are later converted into rock matrix formation factors. The number of data points affected by this is relatively small.

The rock resistivity measurements may have been somewhat affected by the limited measuring range of the in-situ tool, which would give an overestimation of the formation factors in the lower formation factor range. This source of error is judged as minor to insignificant. The mean values and standard deviations of the distributions in Figure 5-2 are shown in Table 5-1 and Table 5-2 for KFM05A and KFM06A, respectively. The in-situ rock matrix formation factor logs of KFM05A and KFM06A are shown in Appendix C1 and C2, respectively.

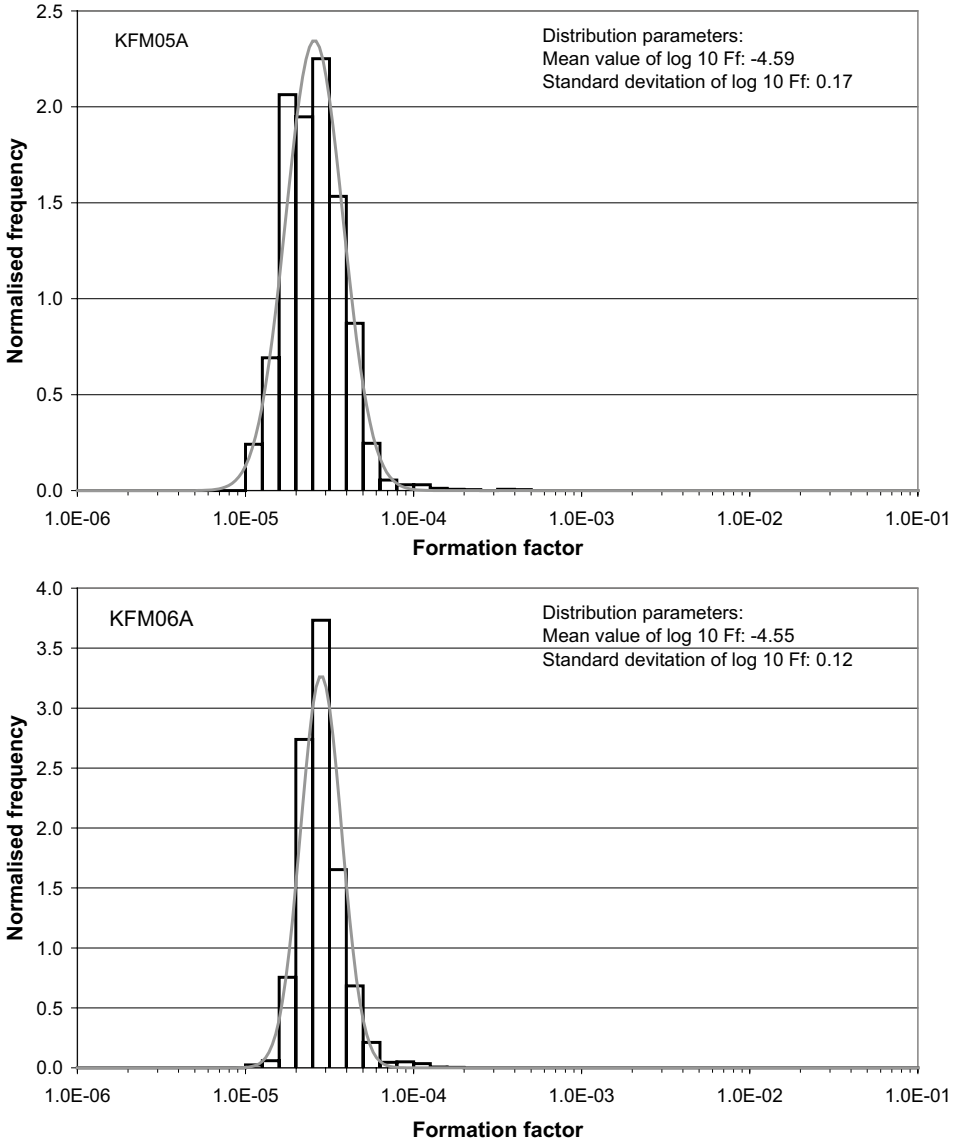

Figure 5-2. *Distributions of in-situ rock matrix formation factors in KFM05A and KFM06A.*

5.3 In-situ fractured rock formation factor

Figure 5-3 shows the distributions of the fractured rock formation factors obtained in-situ in KFM05A and KFM06A.

Except for the deviations in the lower formation factor range that may be due to the limitations of the in-situ rock resistivity tool, a deviation from the log-normal distribution can be seen in the upper formation factor region. Here, some of the obtained formation factors are affected by free water in hydraulically non-conductive fractures. The mean values and standard deviations of the distributions in Figure 5-3 are shown in Table 5-1 and Table 5-2 for KFM05A and KFM06A, respectively. The in-situ fractured rock formation factor logs of KFM05A and KFM06A are shown in Appendix C1 and C2, respectively.

Table 5-2. Distribution parameters and arithmetic mean value of the formation factor, KFM06A.

Formation factor	Number of data points	Mean $\log_{10}(F_f)$	Standard deviation $\log_{10}(F_f)$	Arithmetic mean F_f
In-situ Rock matrix F_f	2,837	–4.55	0.122	2.93×10^{-5}
In-situ Fractured rock F_f	7,957	–4.46	0.207	4.12×10^{-5}

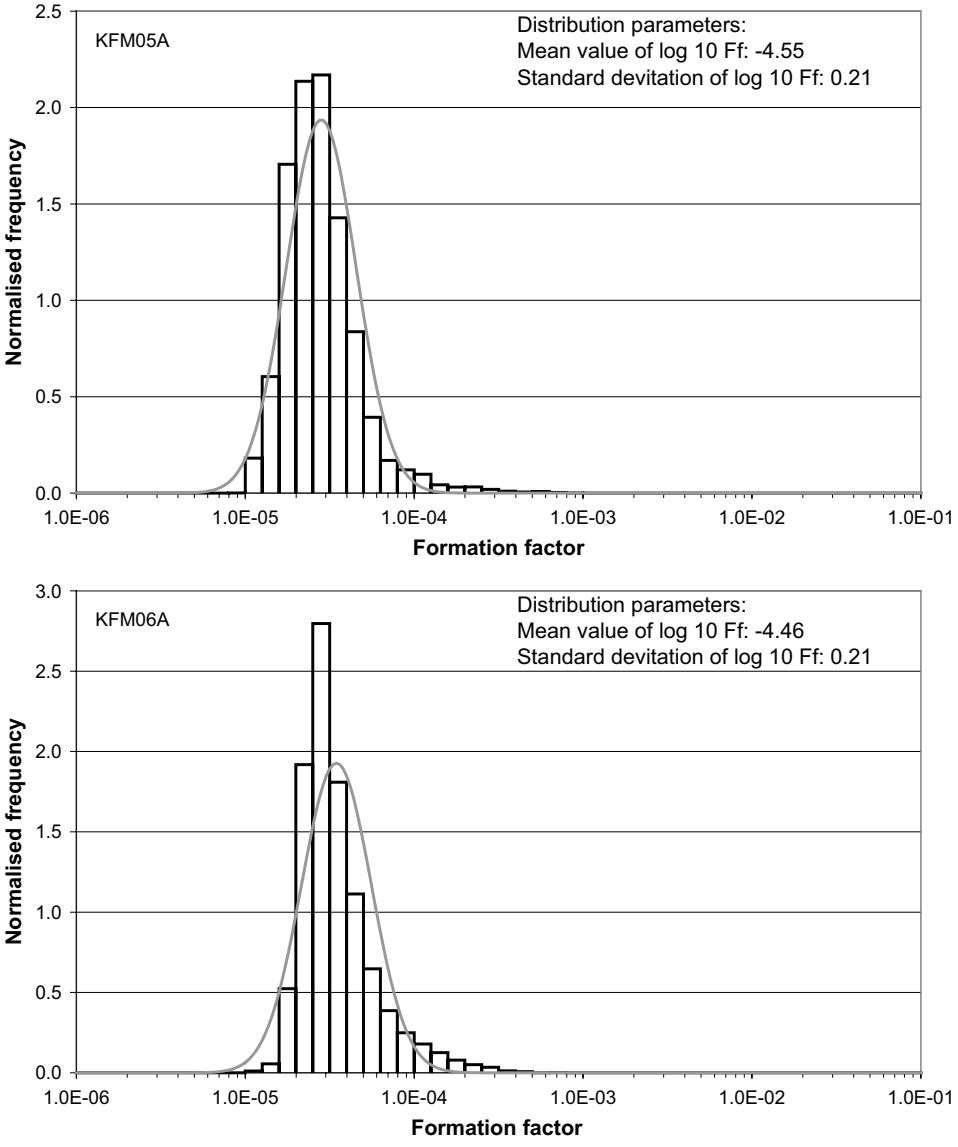

***Figure 5-3**. Distributions of in-situ fractured rock formation factors in KFM05A and KFM06A.*

5.4 Comparison of formation factors of KFM05A

Table 5-1 presents mean values and standard deviations of the log-normal distributions shown in Figures 5-1, 5-2, and 5-3 for KFM05A. In addition, the number of data points obtained and the arithmetic mean values for the different formation factors are shown.

As indicated in Table 5-1, the laboratory formation factors are, on average, almost one order of magnitude larger than those obtained in-situ.

An alternative comparison could be made if comparing each laboratory formation factor with the in-situ rock matrix formation factor, obtained at a corresponding depth. 17 such comparisons are made in made in Appendix C3. The laboratory formation factor from a certain borehole length was compared to the mean value of the in-situ rock matrix formation factors taken within 0.5 m of that borehole length. Here, the laboratory formation factor was on average 7.3 times larger than the rock matrix formation factor.

A reason for the larger laboratory formation factor may be that the rock samples are de-stressed in the laboratory. The laboratory samples may also have been mechanically damaged in the drilling process and sample preparation. In both these cases, results obtained in the laboratory may be non-conservative.

It should also be noted from Table 5-1 that the fractured rock formation factors are, on average, 1.3 times as large as the rock matrix formation factors.

5.5 Comparison of formation factors of KFM06A

Table 5-2 presents mean values and standard deviations of the log-normal distributions shown in Figures 5-2 and 5-3 for KFM06A. In addition, the number of data points obtained and the arithmetic mean values for the different formation factors are shown.

It should be noted from Table 5-2 that the fractured rock formation factors are, on average, 1.4 times as large as the rock matrix formation factors.

6 Summary and discussions

The formation factors obtained in KFM05A and KFM06A range from 9.8×10^{-6} to 9.3×10-4. The formation factors appear to be fairly well distributed according to the log-normal distribution. The obtained in-situ distributions have mean values for log10(Ff) between –4.5 and –4.6 and standard deviations between 0.12 and 0.21. The arithmetic mean values range between 2.8×10^{-5} and 4.1×10^{-5}. In general, similar distributions were obtained.

The fractured rock formation factors were on average 1.3 to 1.4 times as large as the rock matrix formation factors. This indicates that the retention capacity for non-sorbing species due to open, but hydraulically non-conductive, fractures may be significant.

Judging from the obtained formation factor histograms, a small fraction of the obtained in-situ rock resistivities may have been affected by limitations of the in-situ rock resistivity tool.

New data on the pore water chemistry of the rock matrix, obtained by leaching the pore water of core samples in KFM06A /13/, support the approach that the pore water EC can be approximated by the EC of freely flowing groundwater at a corresponding depth. The deviation between the ECs was small compared to the natural variation of the formation factor.

For KFM05A, the formation factors obtained in the laboratory are, on average, almost one order of magnitude larger than those obtained in-situ. This was suggested both by the statistical analysis and by the comparison of laboratory formation factors and in-situ rock matrix formation factors obtained at corresponding depths. This indicates either that the porous system is compressed in-situ or that the laboratory samples become mechanically damaged when brought to the laboratory. In both these cases the laboratory results would be non-conservative.

References

/1/ **Nielsen U.T., Ringgaard J, 2004.** Geophysical borehole logging in borehole KFM05A and HFM19. Site investigation report. SKB P-04-153. Svensk Kärnbränslehantering AB.

/2/ **Nielsen U.T., Ringgaard J, Horn F, 2005.** Geophysical borehole logging in borehole KFM04A, KFM06A, HFM20, HFM21, HFM22 and SP-logging in KFM01A and KFM04A. Site investigation report. SKB P-05-17. Svensk Kärnbränslehantering AB.

/3/ **Pöllänen J, Sokolnicki M, Rouhiainen P, 2004.** Difference flow logging in borehole KFM05A. Site investigation report. SKB P-04-191. Svensk Kärnbränslehantering AB.

/4/ **Rouhiainen P, Sokolnicki M, 2005.** Difference flow logging in borehole KFM06A. Site investigation report. SKB P-05-15. Svensk Kärnbränslehantering AB.

/5/ **Löfgren M, Neretnieks I, 2005.** Formation factor logging in-situ and in the laboratory by electrical methods in KSH01A and KSH02: Measurements and evaluation of methodology. Site investigation report. SKB P-05-27. Svensk Kärnbränslehantering AB.

/6/ **Wacker P, Berg C, Bergelin A, Nilsson A-C, 2005.** Hydrochemical characterisation in KFM05A. Results from an investigated section at 712.6–722.0 m. Site investigation report. SKB P-05-79. Svensk Kärnbränslehantering AB.

/7/ **Berg C, Wacker P, Nilsson A-C, 2005.** Chemical characterisation in borehole KFM06A. Results from the investigated sections at 266.0–271.0 m, 353.5–360.6 m and 768.0–775.1 m. Site investigation report. SKB P-05-178. Svensk Kärnbränslehantering AB.

/8/ **Petersson J, Berglund J, Wängnerud A, Danielsson P, Stråhle A, 2004**. Boremap mapping of telescopic drilled borehole KFM05A. Site investigation report. SKB P-04-295. Svensk Kärnbränslehantering AB.

/9/ **Petersson J, Skogsmo G, Berglund J , Wängnerud A, Stråhle A, 2005**. Boremap mapping of telescopic drilled borehole KFM06A and core drilled borehole KFM06B. Site investigation report. SKB P-05-101. Svensk Kärnbränslehantering AB.

/10/ **Ehrenborg J, Vladislav S, 2004**. Boremap mapping of core drilled boreholes KSH01A and KSH01B. Site investigation report. SKB P-04-01. Svensk Kärnbränslehantering AB.

/11/ **Löfgren M, Neretnieks I, 2002.** Formation factor logging in-situ by electrical methods. Background and methodology. SKB TR-02-27. Svensk Kärnbränslehantering AB.

/12/ **Löfgren M, 2001.** Formation factor logging in igneous rock by electrical methods. Licentiate thesis at the Royal Institute of Technology, Stockholm, Sweden. ISBN 91-7283-207-X.

/13/ **Waber H N, Smellie J A T, 2005.** Borehole KFM06A: Characterisation of pore water. Part 1: Diffusion experiments. Site investigation report. SKB P-05-196. Svensk Kärnbränslehantering AB.

/14/ **Ohlsson Y, 2000.** Studies of Ionic Diffusion in Crystalline Rock. Doctoral thesis at the Royal Institute of Technology, Stockholm, Sweden. ISBN 91-7283-025-5.

/15/ **Löfgren M, 2004.** Diffusive properties of granitic rock as measured by in-situ electrical methods. Doctoral thesis at the Royal Institute of Technology, Stockholm, Sweden. ISBN 91-7283-935-X.

/16/ **Laaksoharju M, Gimeno M, Auqué L, Gómez J, Smellie J, Tullborg E-L, Gurban I, 2004.** Hydrogeochemical evaluation of the Forsmark site, model version 1.1. SKB R-04-05. Svensk Kärnbränslehantering AB.

/17/ **Thunehed H, 2005.** Resistivity measurements and determination of formation factors on samples from KFM03A, KFM04A and KFM05A. Site investigation report. SKB P-05-76. Svensk Kärnbränslehantering AB.

/18/ **Johnson RA, 1994.** Miller and Freund's probability and statistics for engineers, 5ed. Prentice-Hall Inc. ISBN 0-13-721408-1.

/19/ **Löfgren M, Neretnieks I, 2005.** Formation factor logging in-situ by electrical methods in KFM03A and KFM04A. Site investigation report. SKB P-05-108. Svensk Kärnbränslehantering AB.

Appendix A

Appendix A1: Laboratory formation factor for rock samples from KFM05A

Secup (m)	Formation factor
208.835	7.09E–05
228.145	1.39E–04
249.045	2.91E–04
269.675	1.69E–04
288.865	1.48E–04
308.565	1.61E–04
348.265	1.81E–04
388.945	1.68E–04
408.765	1.36E–04
428.95	4.09E–05
449.365	1.32E–04
469.845	3.52E–04
489.375	3.57E–04
509.085	7.01E–04
528.735	1.22E–04
548.555	1.39E–04
590.065	1.27E–04
629.315	2.64E–04
650.435	1.46E–04
669.915	8.17E–05
689.705	1.13E–04
700.295	4.38E–04
739.835	2.48E–04

Secup = upper position in borehole for sample.

Appendix B

Appendix B1: In-situ rock resistivities and fractures KFM05

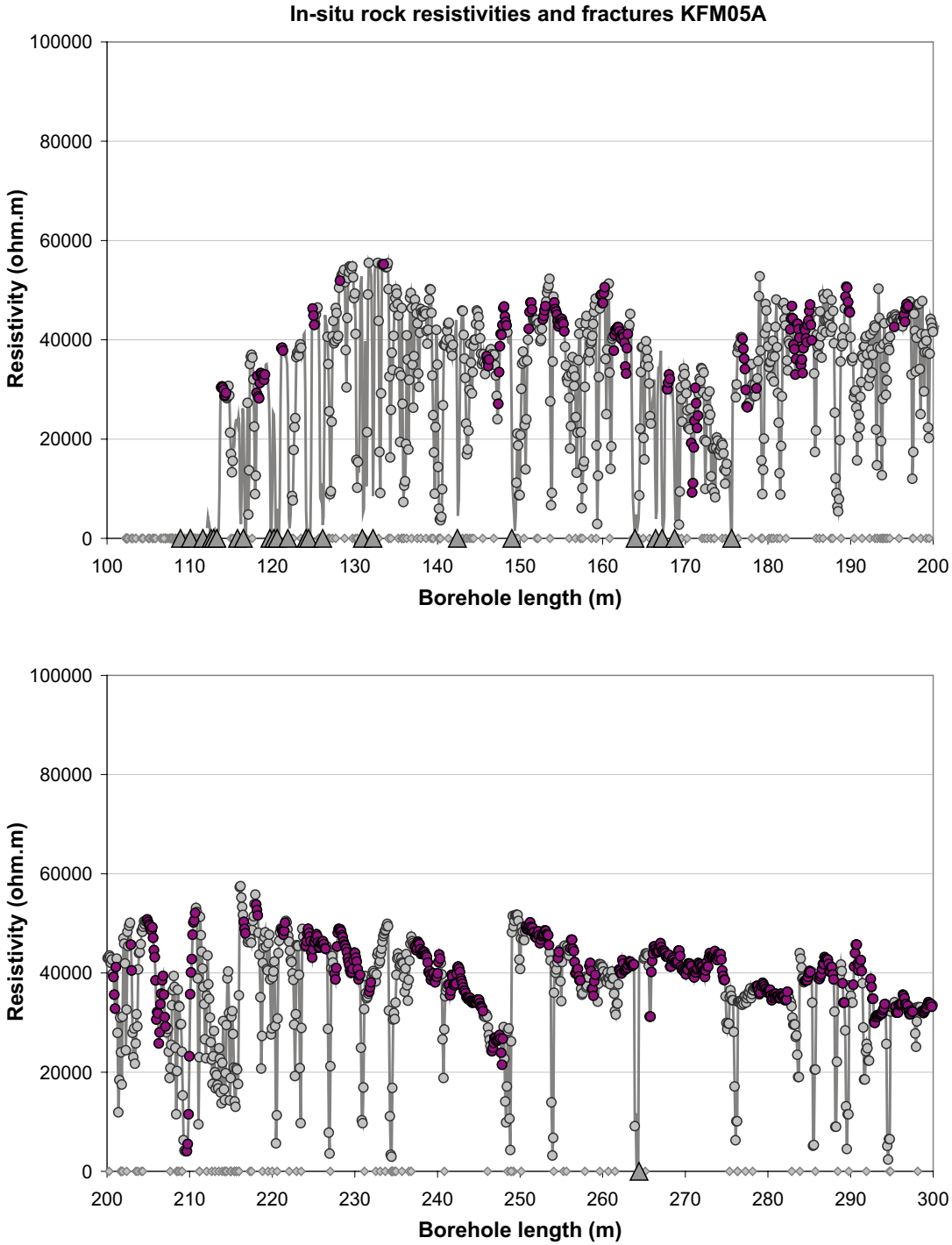

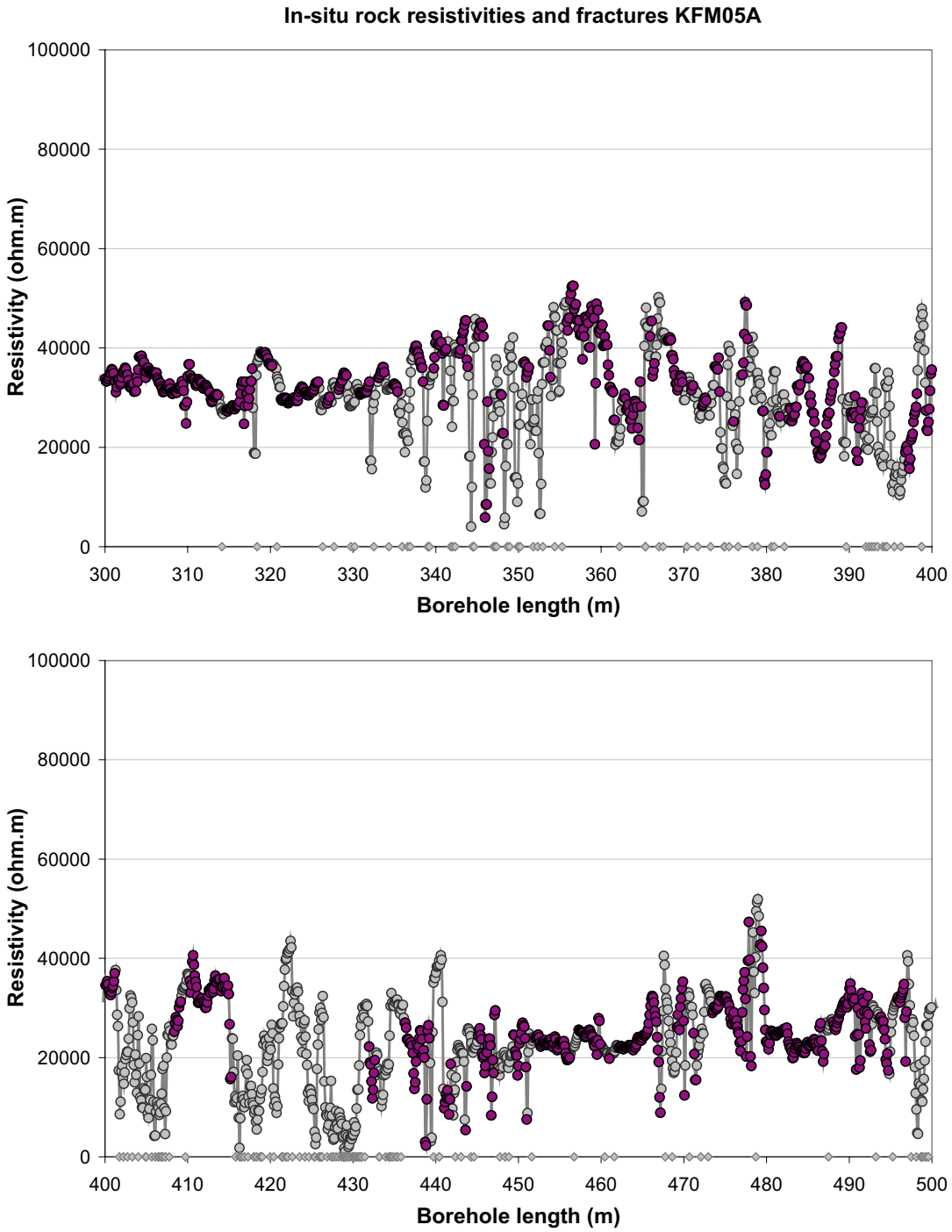
In-situ rock resistivities and fractures KFM05A
Resistivity (ohm.m)
100000
80000
60000
40000
20000
0
300
310
320
330
340
350
360
370
380
390
400
Borehole length (m)
Resistivity (ohm.m)
100000
80000
60000
40000
20000
0
400
410
420
430
440
450
460
470
480
490
500
Borehole length (m)
Rock resistivity
Fractured rock resistivity
Rock matrix resistivity
Location of broken fracture parting the drill core
Location of hydraulically conductive fracture detected in the difference flow logging

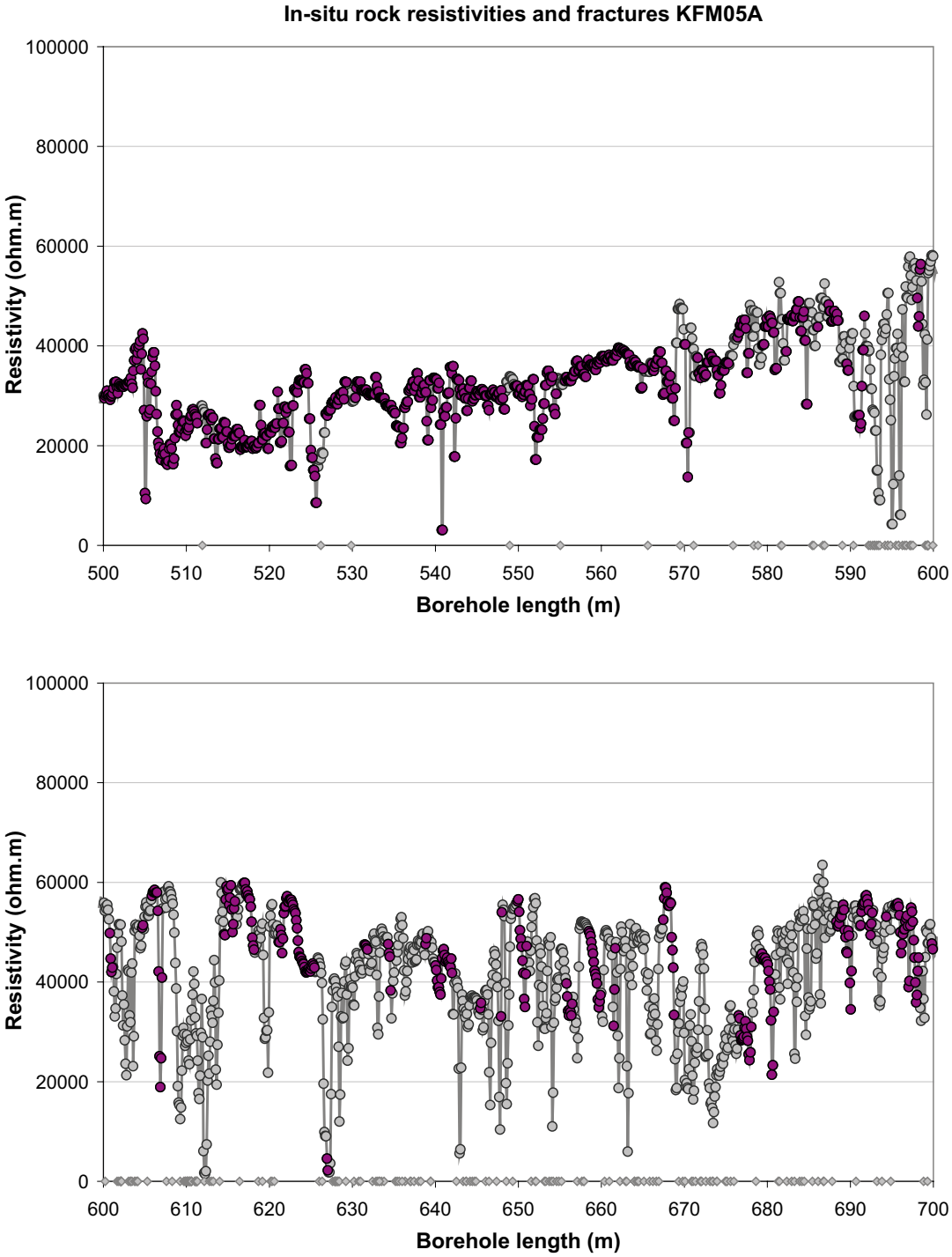
In-situ rock resistivities and fractures KFM05A
Resistivity (ohm.m)
100000
80000
60000
40000
20000
0
500
510
520
530
540
550
560
570
580
590
600
Borehole length (m)
Resistivity (ohm.m)
100000
80000
60000
40000
20000
0
600
610
620
630
640
650
660
670
680
690
700
Borehole length (m)
Rock resistivity
Fractured rock resistivity
Rock matrix resistivity
Location of broken fracture parting the drill core
Location of hydraulically conductive fracture detected in the difference flow logging

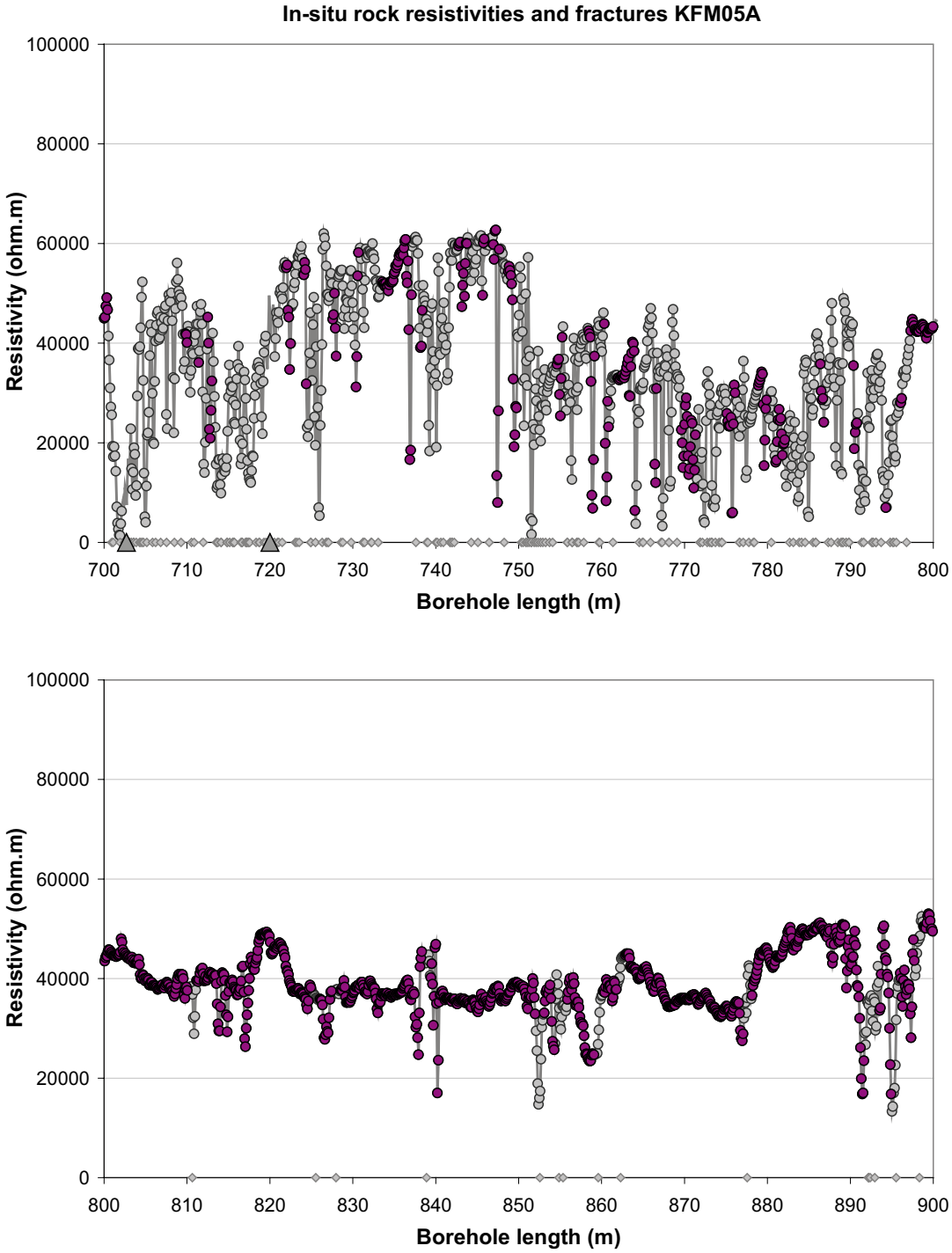
In-situ rock resistivities and fractures KFM05A
Resistivity (ohm.m)
100000
80000
60000
40000
20000
0
700
710
720
730
740
750
760
770
780
790
800
Borehole length (m)
Resistivity (ohm.m)
100000
80000
60000
40000
20000
0
800
810
820
830
840
850
860
870
880
890
900
Borehole length (m)
Rock resistivity
Fractured rock resistivity
Rock matrix resistivity
Location of broken fracture parting the drill core
Location of hydraulically conductive fracture detected in the difference flow logging

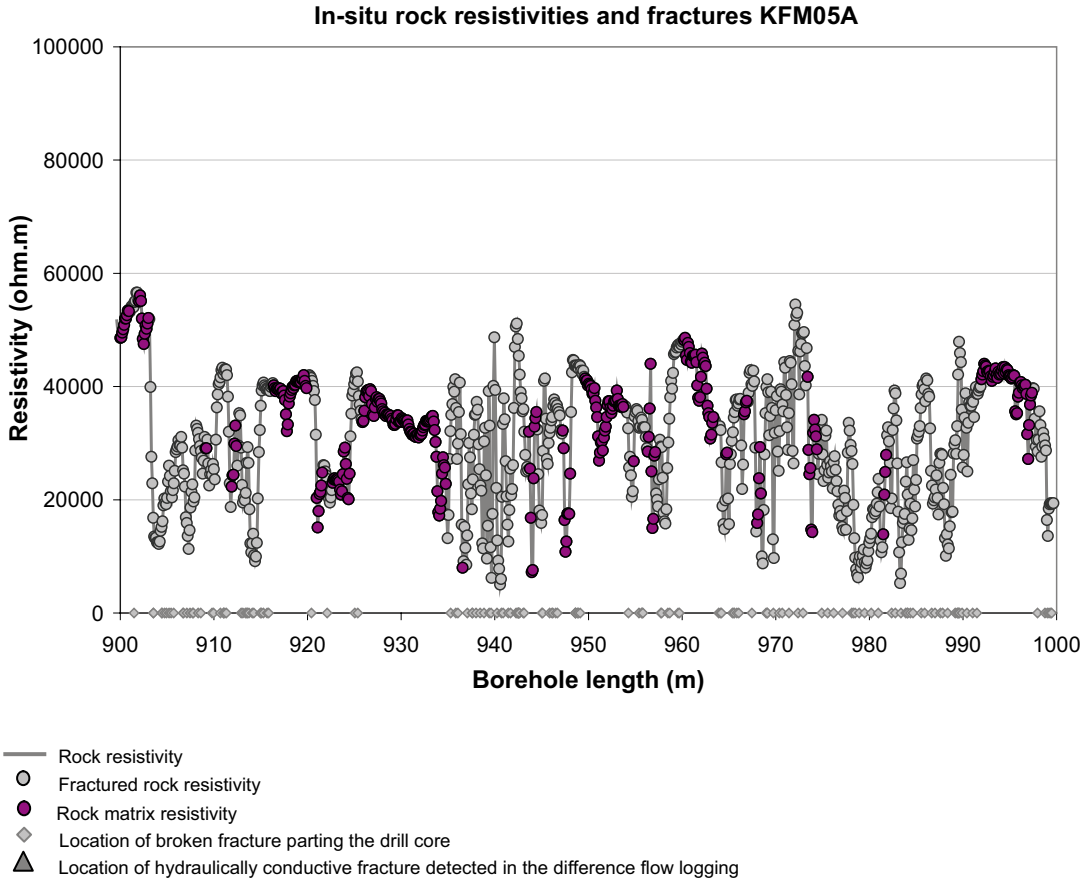
In-situ rock resistivities and fractures KFM05A
Resistivity (ohm.m)
100000
80000
60000
40000
20000
0
900
910
920
930
940
950
960
970
980
990
1000
Borehole length (m)
Rock resistivity
Fractured rock resistivity
Rock matrix resistivity
Location of broken fracture parting the drill core
Location of hydraulically conductive fracture detected in the difference flow logging

Appendix B2: In-situ rock resistivities and fractures KFM06A

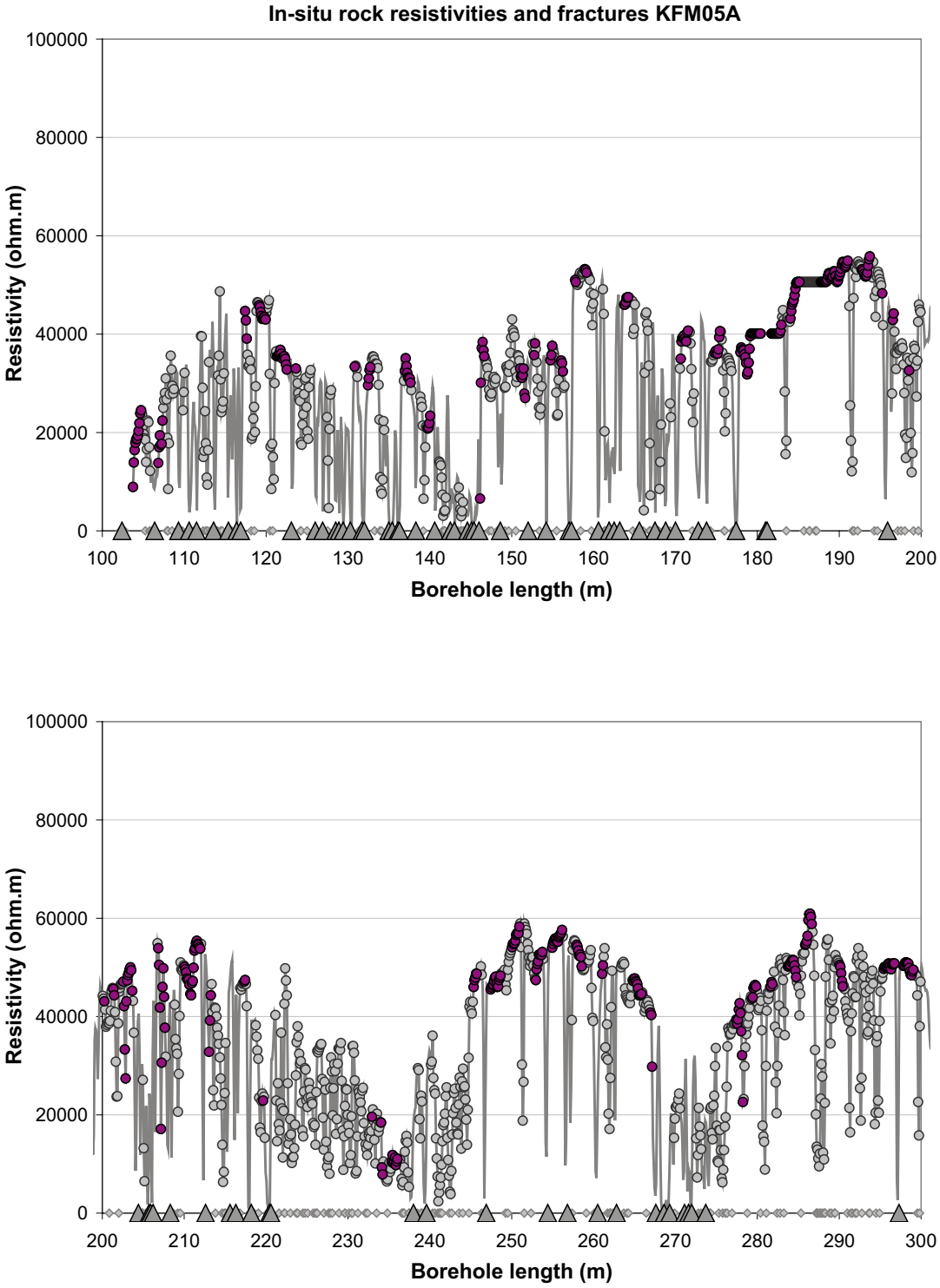

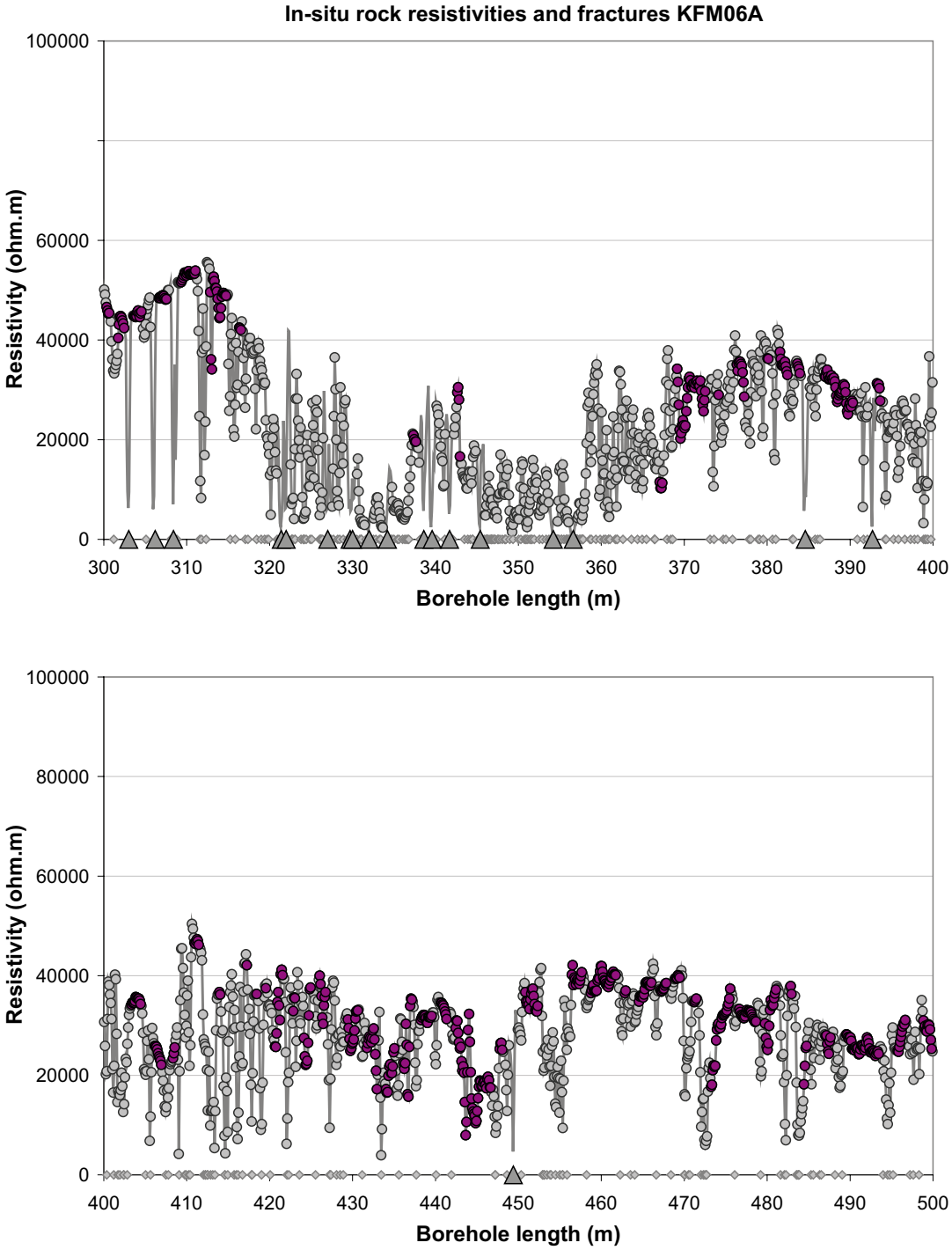
In-situ rock resistivities and fractures KFM06A
Resistivity (ohm.m)
100000
60000
40000
20000
0
300
310
320
330
340
350
360
370
380
390
400
Borehole length (m)
Resistivity (ohm.m)
100000
80000
60000
40000
20000
0
400
410
420
430
440
450
460
470
480
490
500
Borehole length (m)
Rock resistivity
Fractured rock resistivity
Rock matrix resistivity
Location of broken fracture parting the drill core
Location of hydraulically conductive fracture detected in the difference flow logging

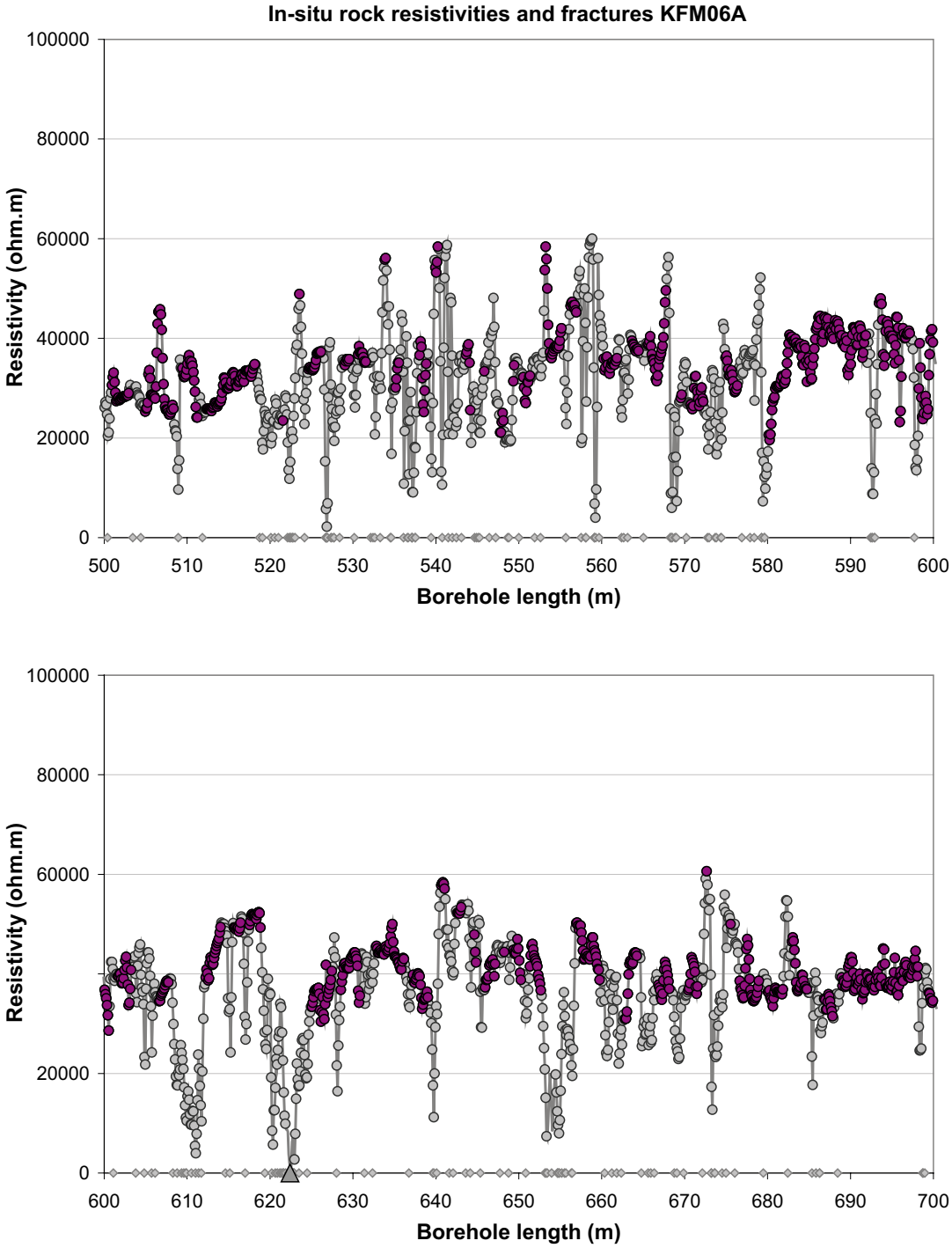
In-situ rock resistivities and fractures KFM06A
Resistivity (ohm.m)
100000
80000
60000
40000
20000
0
500
510
520
530
540
550
560
570
580
590
600
Borehole length (m)
Resistivity (ohm.m)
100000
80000
60000
20000
0
600
610
620
630
640
650
660
670
680
690
700
Borehole length (m)
Rock resistivity
Fractured rock resistivity
Rock matrix resistivity
Location of broken fracture parting the drill core
Location of hydraulically conductive fracture detected in the difference flow logging

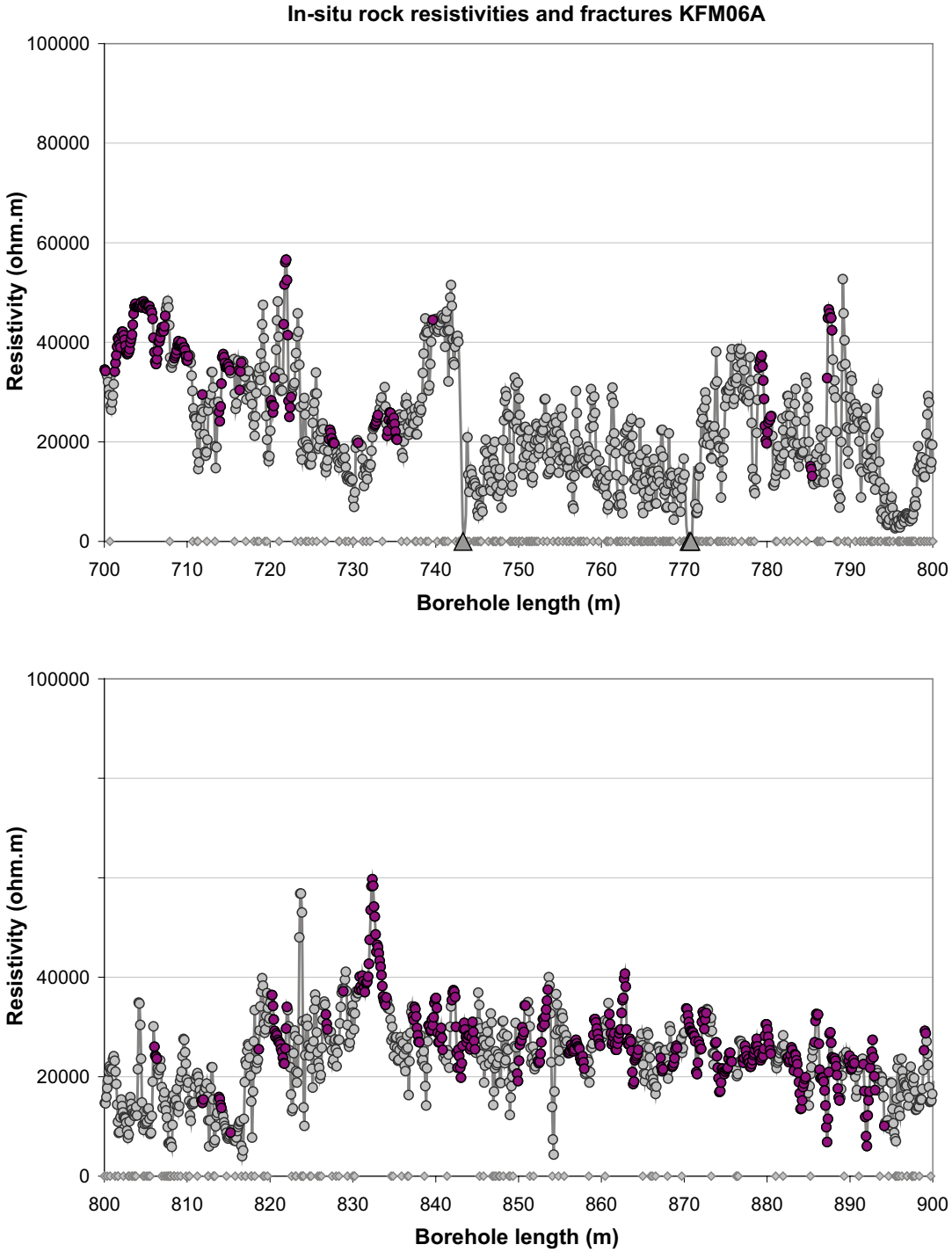
In-situ rock resistivities and fractures KFM06A
Resistivity (ohm.m)
100000
80000
60000
40000
20000
0
700
710
720
730
740
750
760
770
780
790
800
Borehole length (m)
Resistivity (ohm.m)
100000
40000
20000
0
800
810
820
830
840
850
860
870
880
890
900
Borehole length (m)
Rock resistivity
Fractured rock resistivity
Rock matrix resistivity
Location of broken fracture parting the drill core
Location of hydraulically conductive fracture detected in the difference flow logging

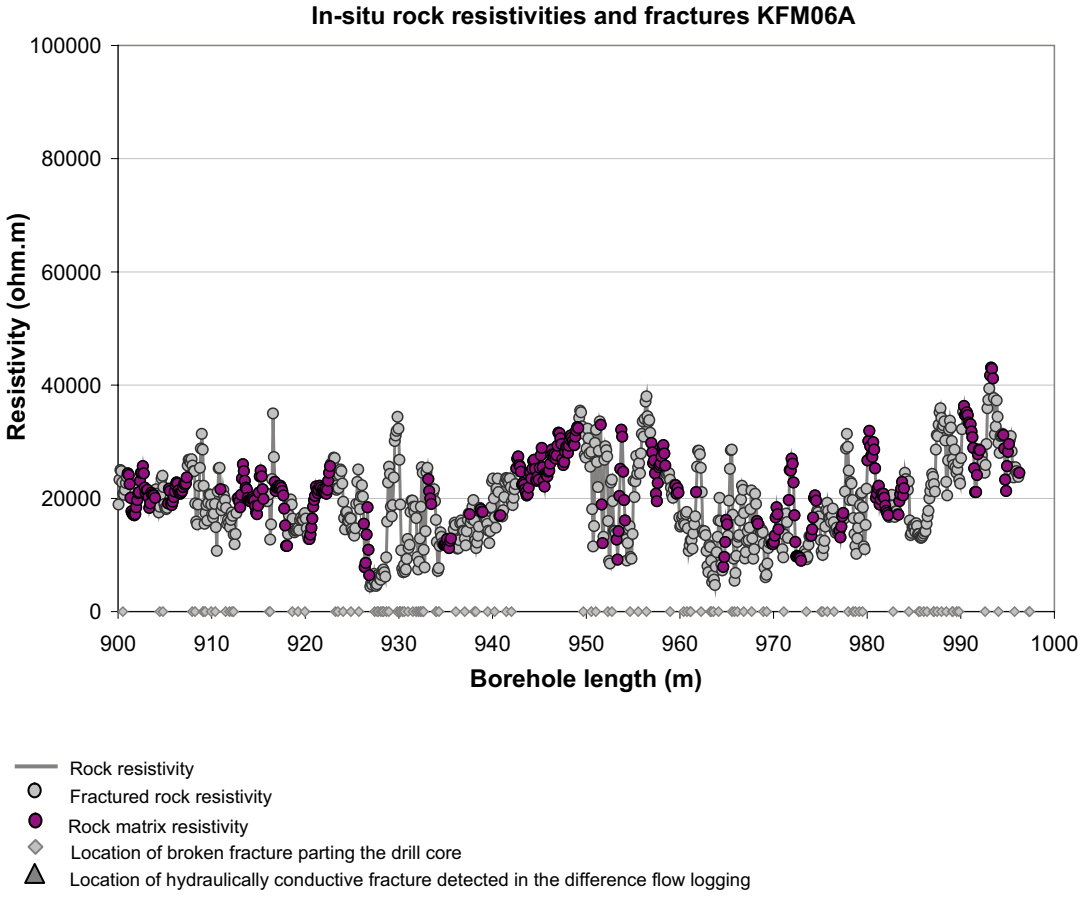
In-situ rock resistivities and fractures KFM06A
Resistivity (ohm.m)
100000
80000
60000
40000
20000
0
900
910
920
930
940
950
960
970
980
990
1000
Borehole length (m)
Rock resistivity
Fractured rock resistivity
Rock matrix resistivity
Location of broken fracture parting the drill core
Location of hydraulically conductive fracture detected in the difference flow logging

Appendix C

Appendix C1: In-situ and laboratory formation factors KFM05A

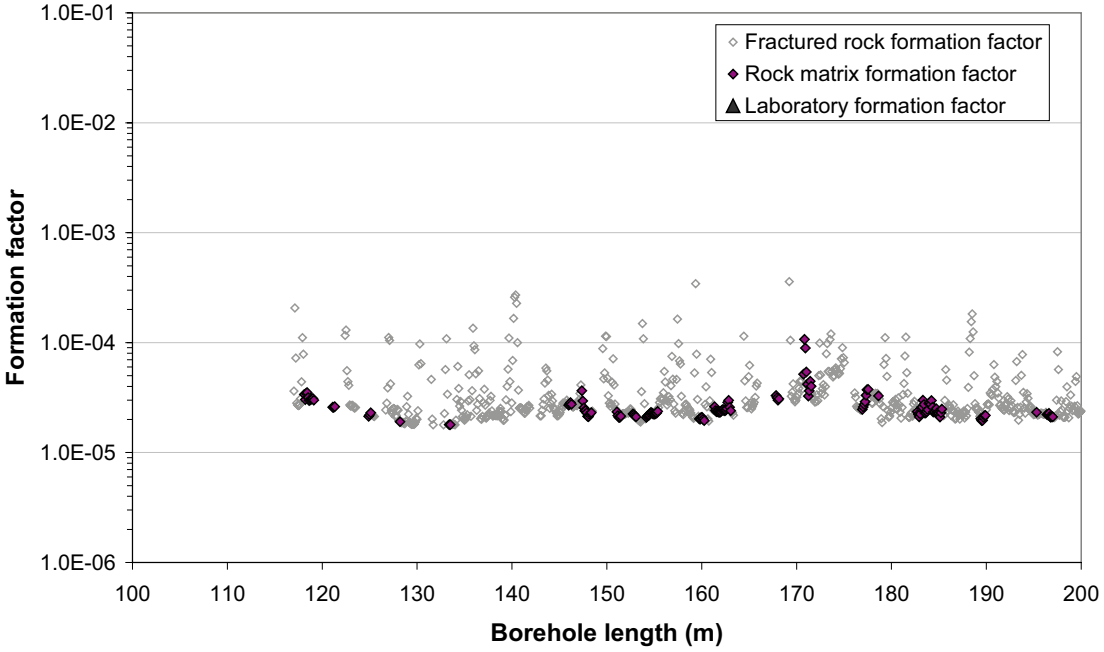

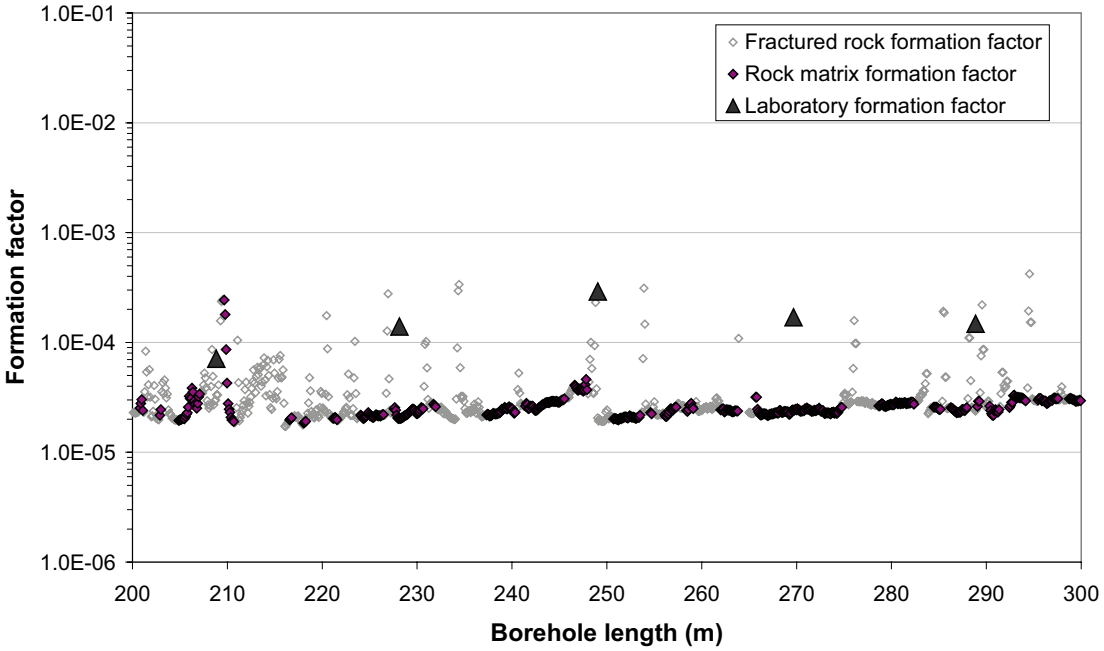

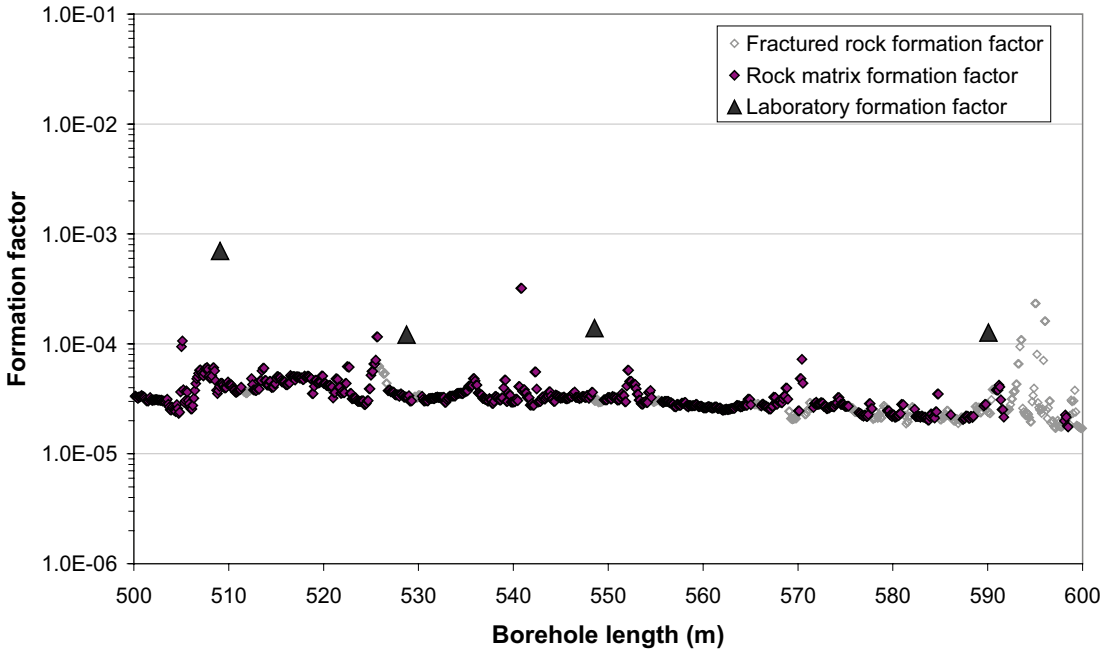
Fractured rock formation factor
Rock matrix formation factor
Laboratory formation factor
Formation factor
1.0E-01
1.0E-02
1.0E-03
1.0E-04
1.0E-05
1.0E-06
500
510
520
530
540
550
560
570
580
590
600
Borehole length (m)

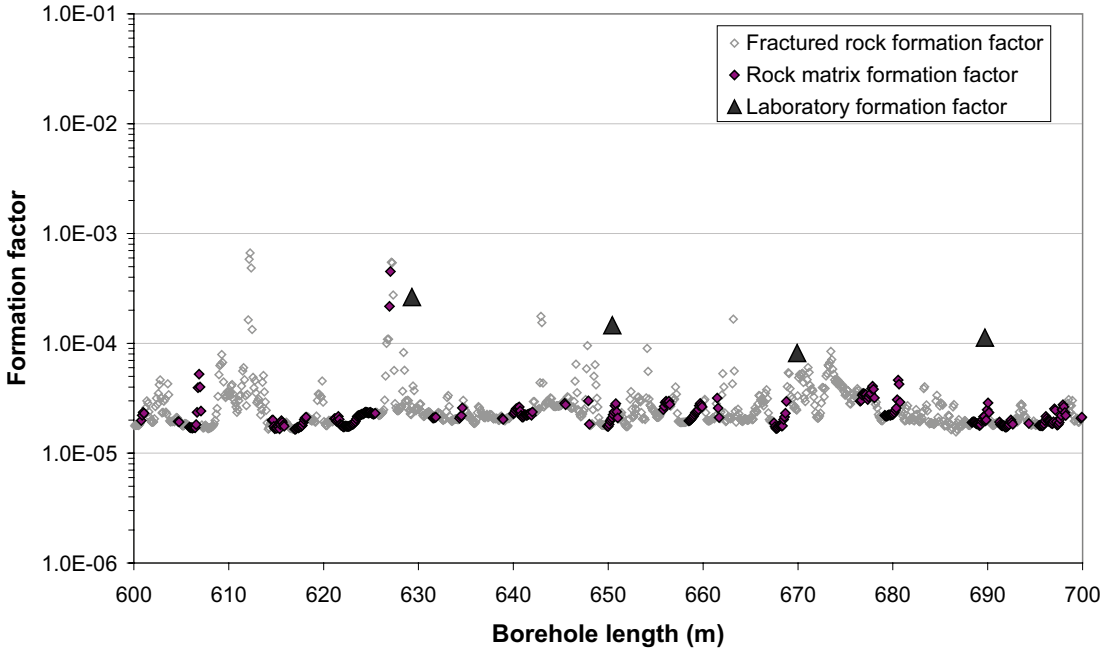
Fractured rock formation factor
Rock matrix formation factor
Laboratory formation factor
Formation factor
1.0E-01
1.0E-02
1.0E-03
1.0E-04
1.0E-05
1.0E-06
600
610
620
630
640
650
660
670
680
690
700
Borehole length (m)

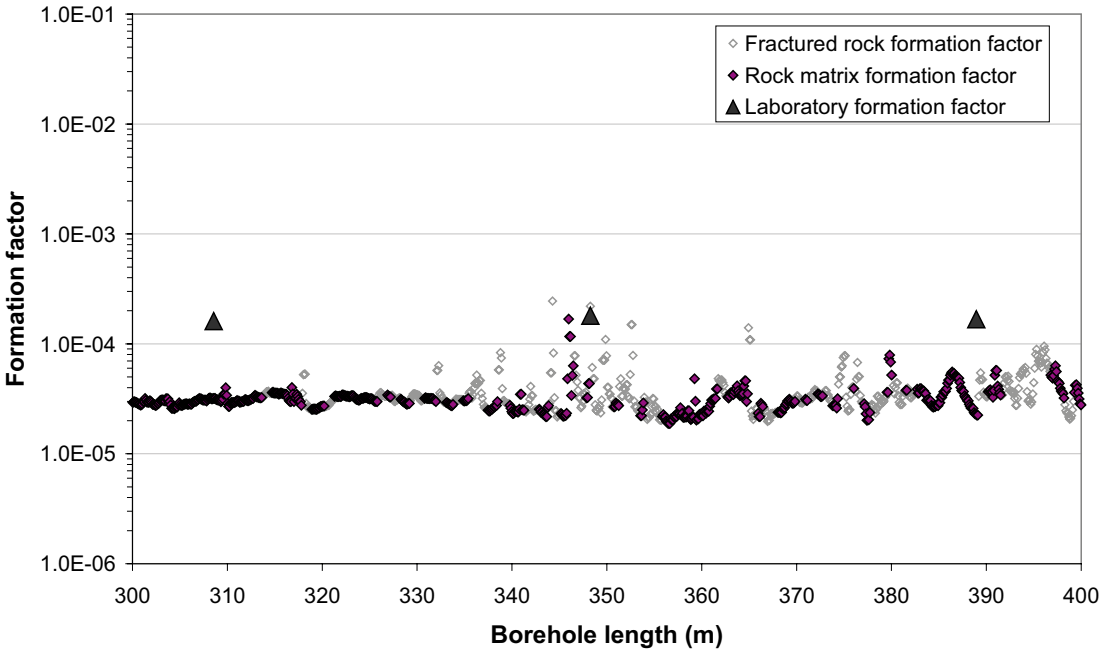
Fractured rock formation factor
Rock matrix formation factor
Laboratory formation factor
Formation factor
1.0E-01
1.0E-02
1.0E-03
1.0E-04
1.0E-05
1.0E-06
300
310
320
330
340
350
360
370
380
390
400
Borehole length (m)

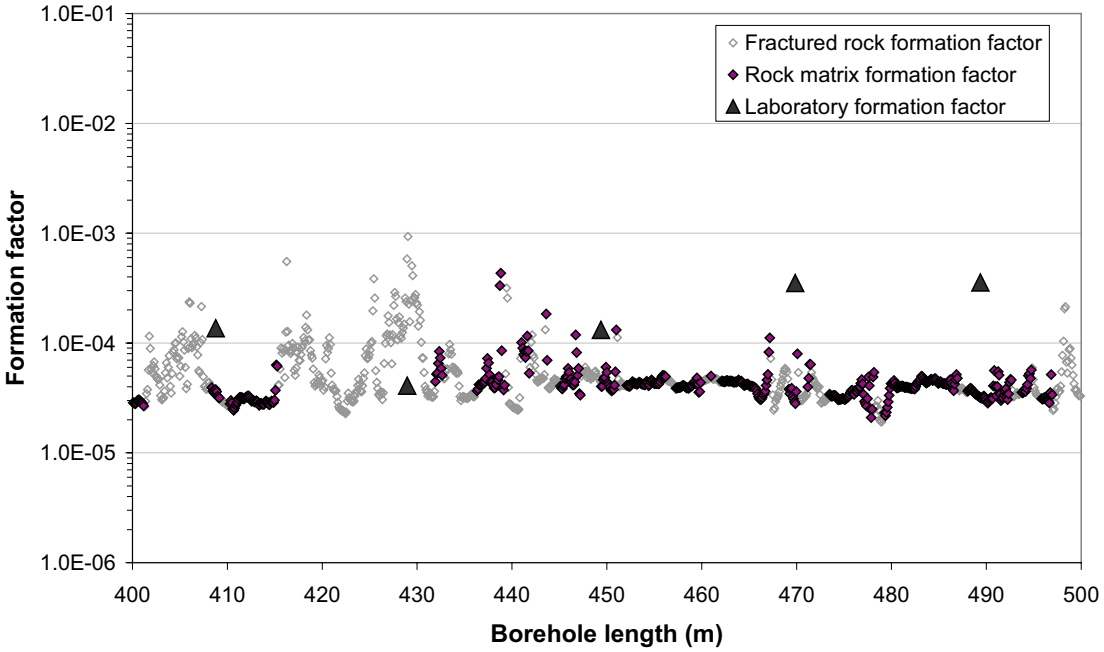
Fractured rock formation factor
Rock matrix formation factor
Laboratory formation factor
Formation factor
1.0E-01
1.0E-02
1.0E-03
1.0E-04
1.0E-05
1.0E-06
400
410
420
430
440
450
460
470
480
490
500
Borehole length (m)

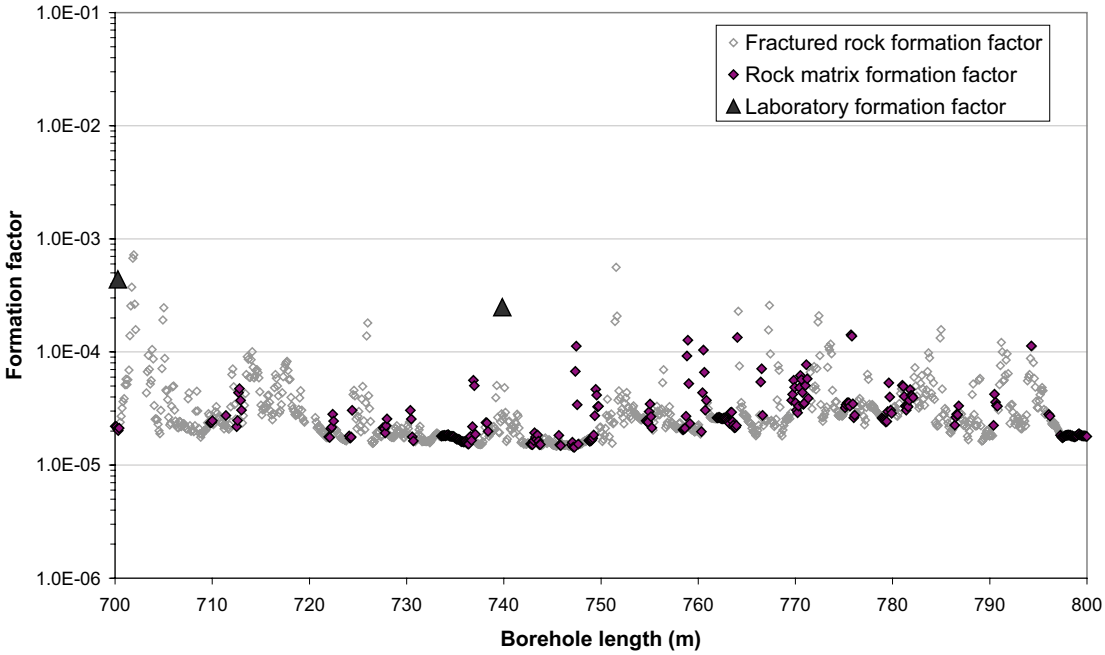
Fractured rock formation factor
Rock matrix formation factor
Laboratory formation factor
Formation factor
1.0E-01
1.0E-02
1.0E-03
1.0E-04
1.0E-05
1.0E-06
700
710
720
730
740
750
760
770
780
790
800
Borehole length (m)

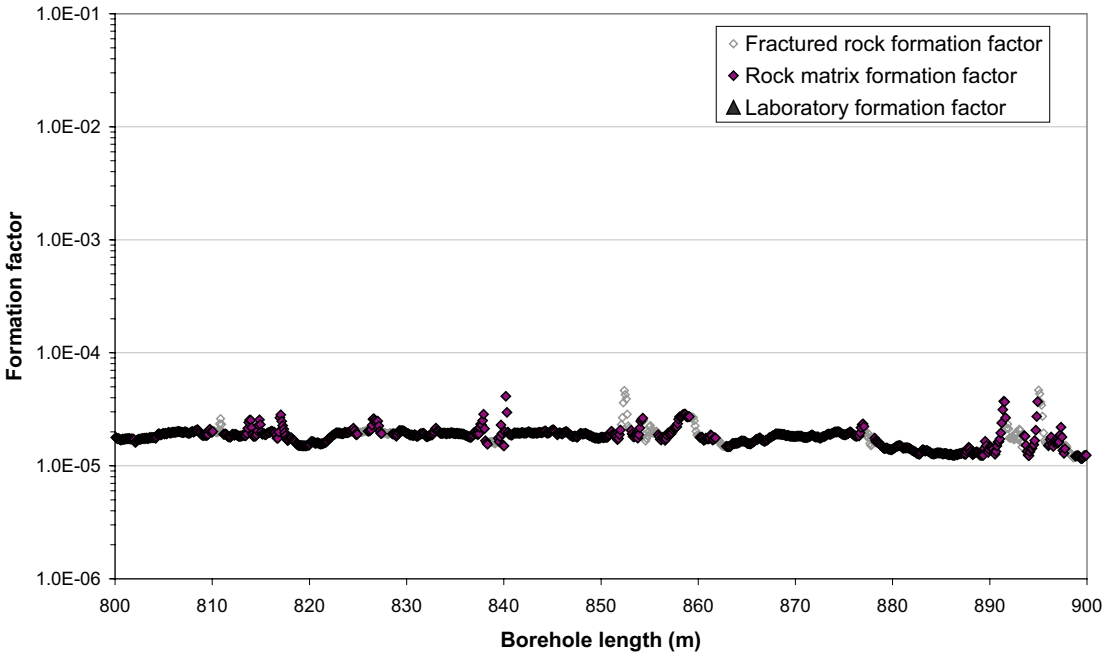
Fractured rock formation factor
Rock matrix formation factor
Laboratory formation factor
Formation factor
1.0E-01
1.0E-02
1.0E-03
1.0E-04
1.0E-05
1.0E-06
800
810
820
830
840
850
860
870
880
890
900
Borehole length (m)

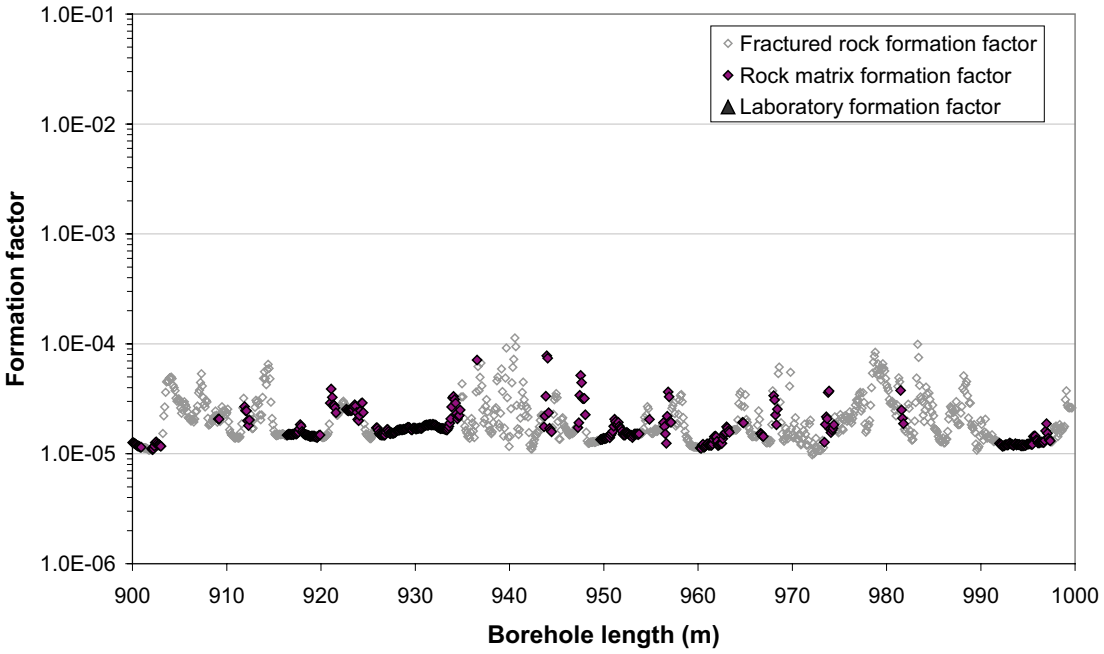
Fractured rock formation factor
Rock matrix formation factor
Laboratory formation factor
Formation factor
1.0E-01
1.0E-02
1.0E-03
1.0E-04
1.0E-05
1.0E-06
900
910
920
930
940
950
960
970
980
990
1000
Borehole length (m)

Appendix C2: In-situ and laboratory formation factors KFM06A

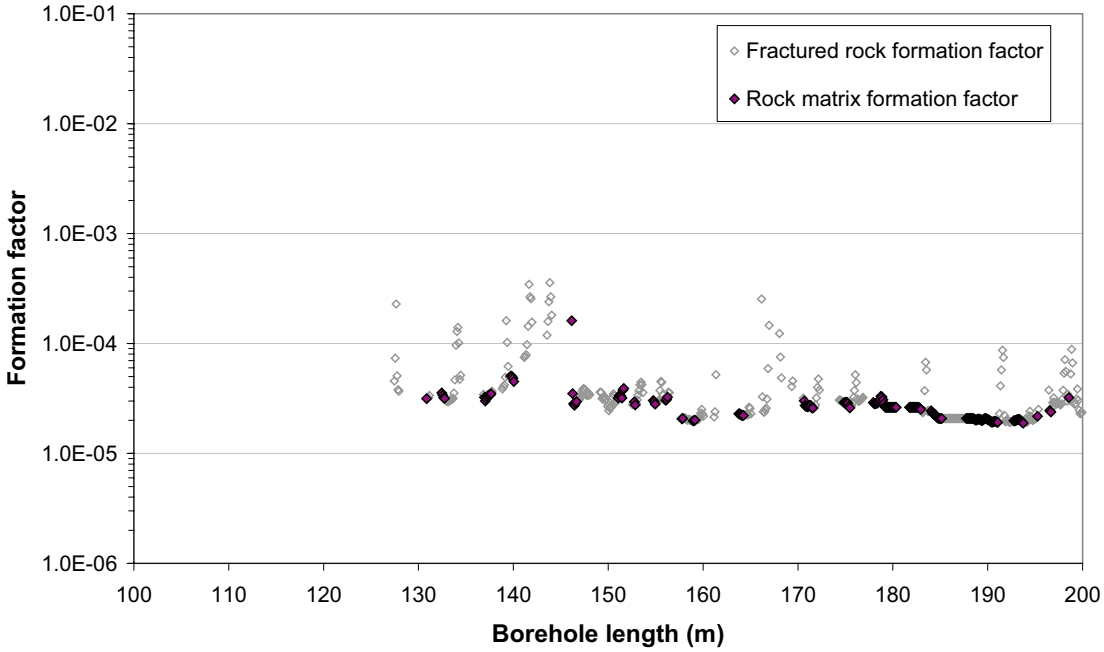

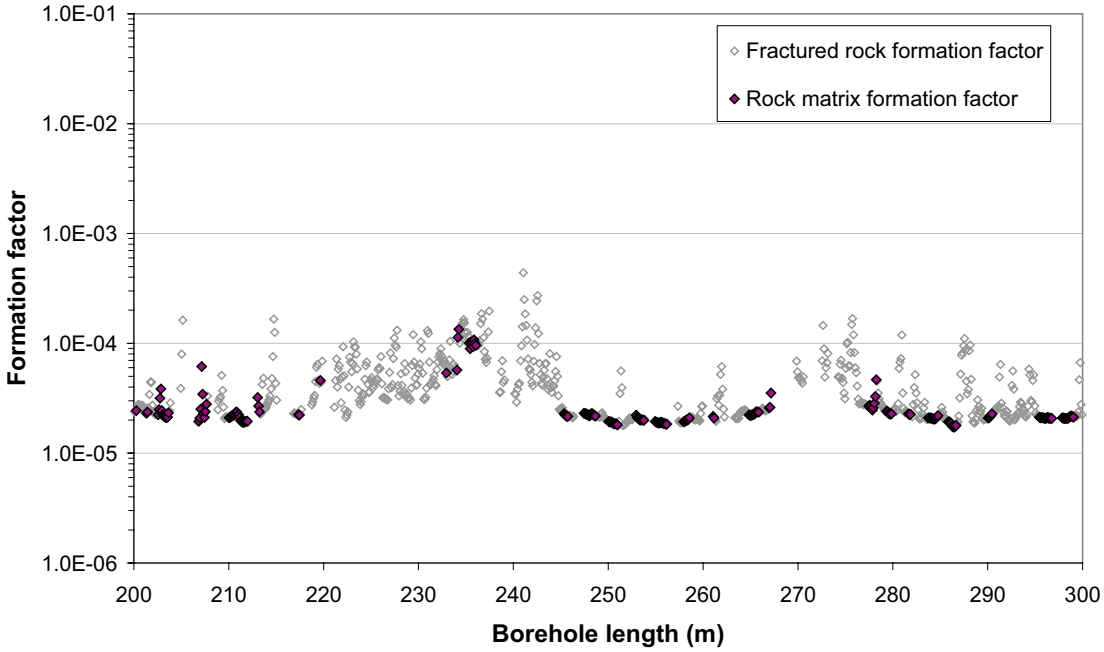

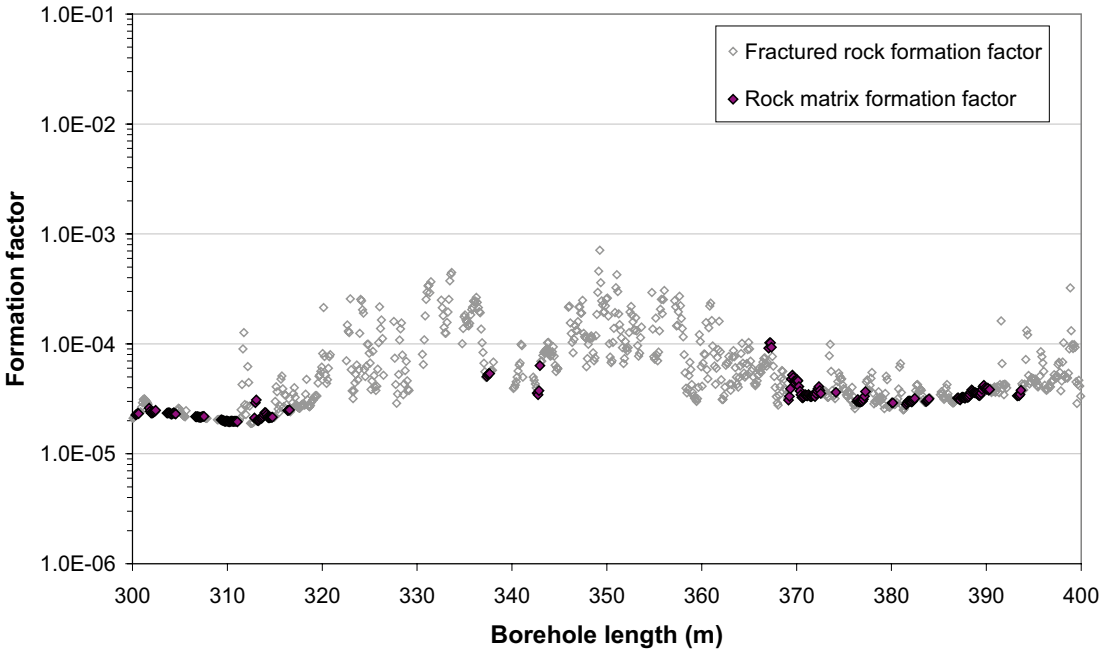
Fractured rock formation factor
Rock matrix formation factor
Formation factor
1.0E-01
1.0E-02
1.0E-03
1.0E-04
1.0E-05
1.0E-06
300
310
320
330
340
350
360
370
380
390
400
Borehole length (m)

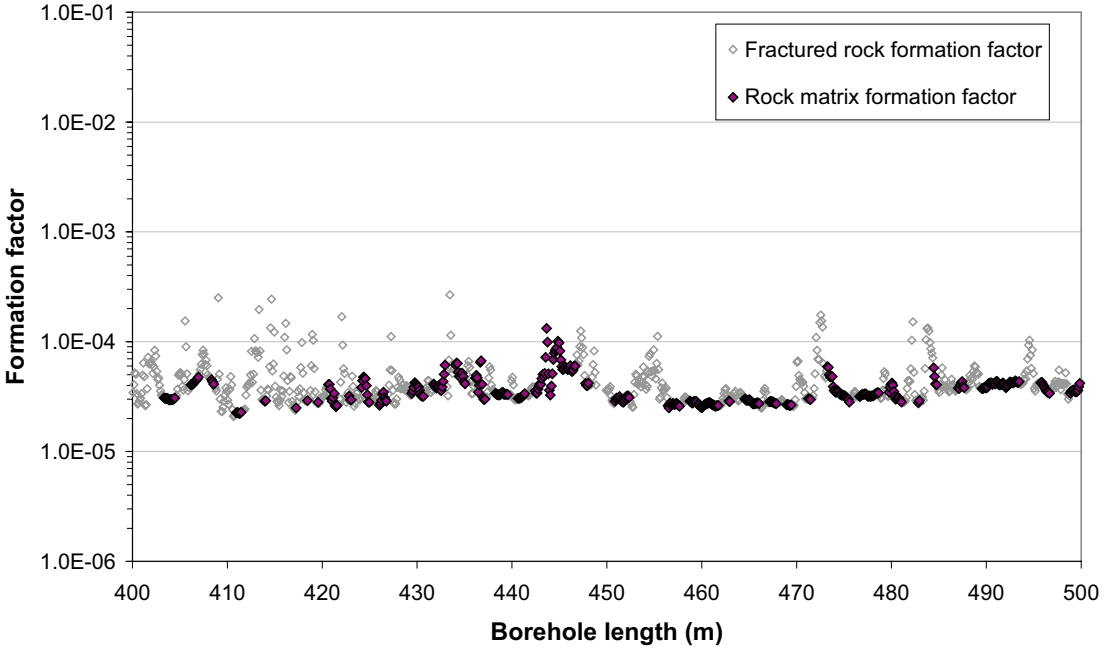
Fractured rock formation factor
Rock matrix formation factor
Formation factor
1.0E-01
1.0E-02
1.0E-03
1.0E-04
1.0E-05
1.0E-06
400
410
420
430
440
450
460
470
480
490
500
Borehole length (m)

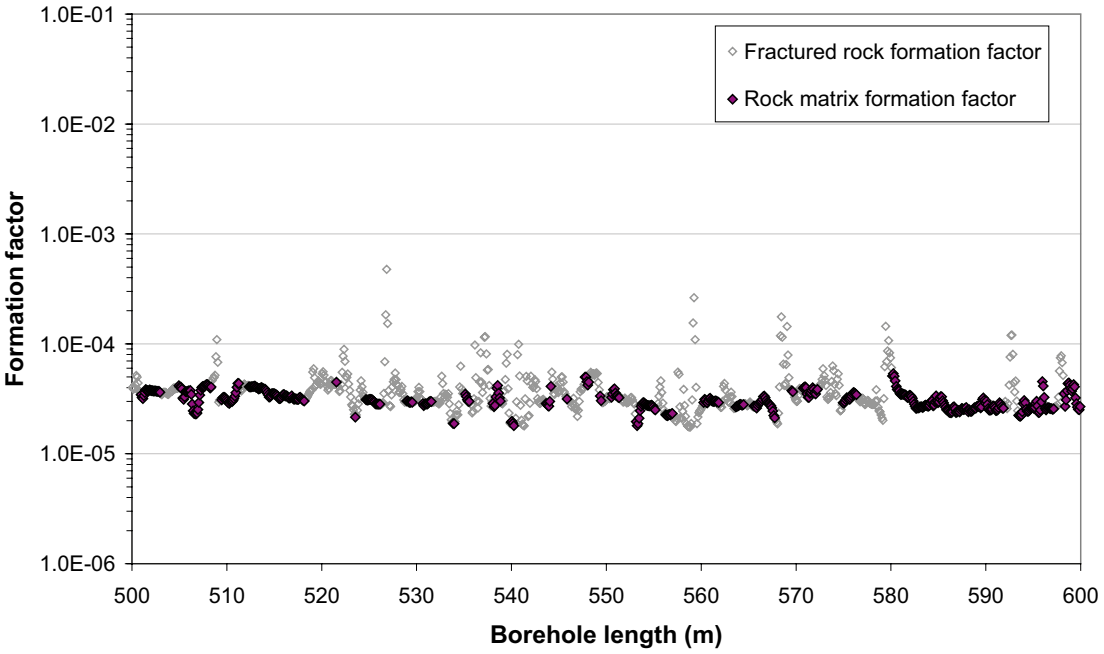
Fractured rock formation factor
Rock matrix formation factor
Formation factor
1.0E-01
1.0E-02
1.0E-03
1.0E-04
1.0E-05
1.0E-06
500
510
520
530
540
550
560
570
580
590
600
Borehole length (m)

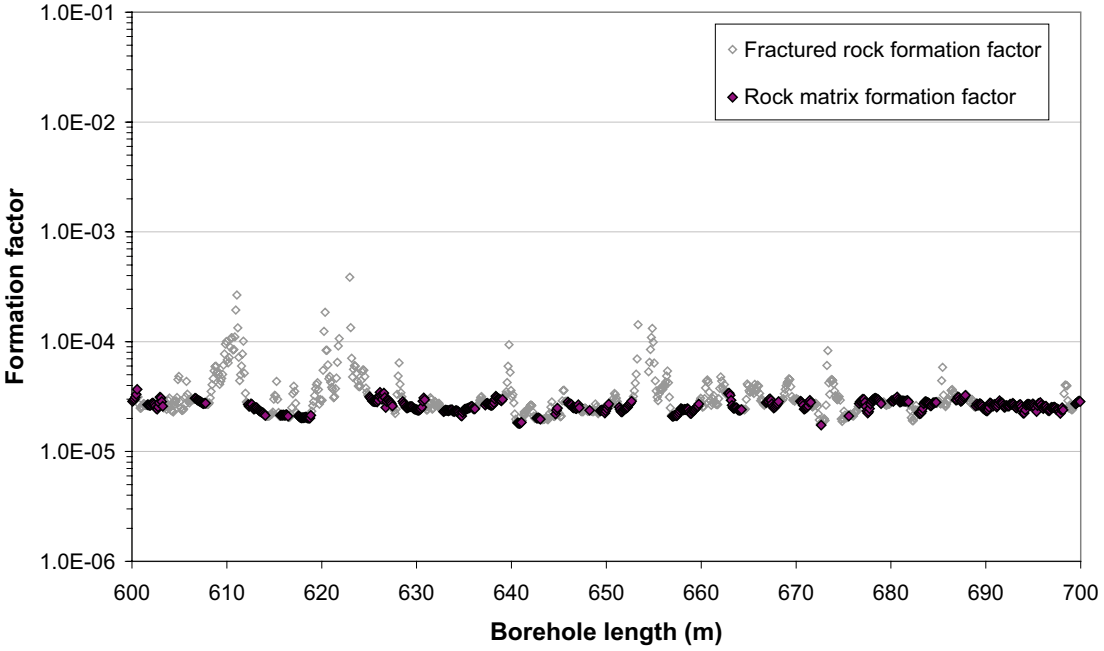
Fractured rock formation factor
Rock matrix formation factor
Formation factor
1.0E-01
1.0E-02
1.0E-03
1.0E-04
1.0E-05
1.0E-06
600
610
620
630
640
650
660
670
680
690
700
Borehole length (m)

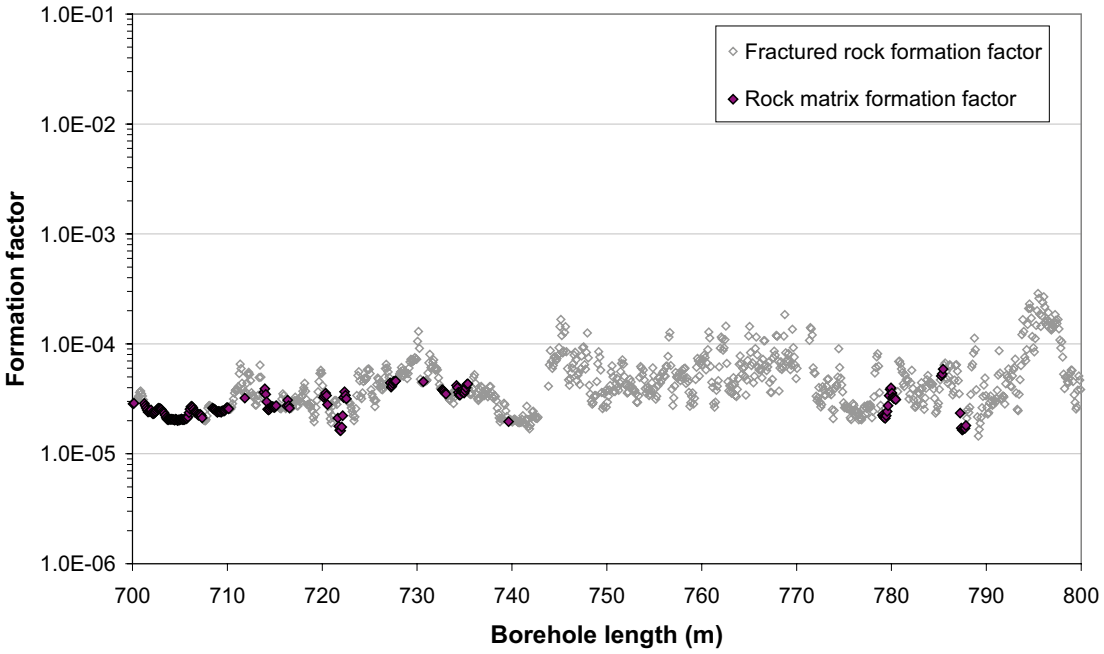
Fractured rock formation factor
Rock matrix formation factor
Formation factor
1.0E-01
1.0E-02
1.0E-03
1.0E-04
1.0E-05
1.0E-06
700
710
720
730
740
750
760
770
780
790
800
Borehole length (m)

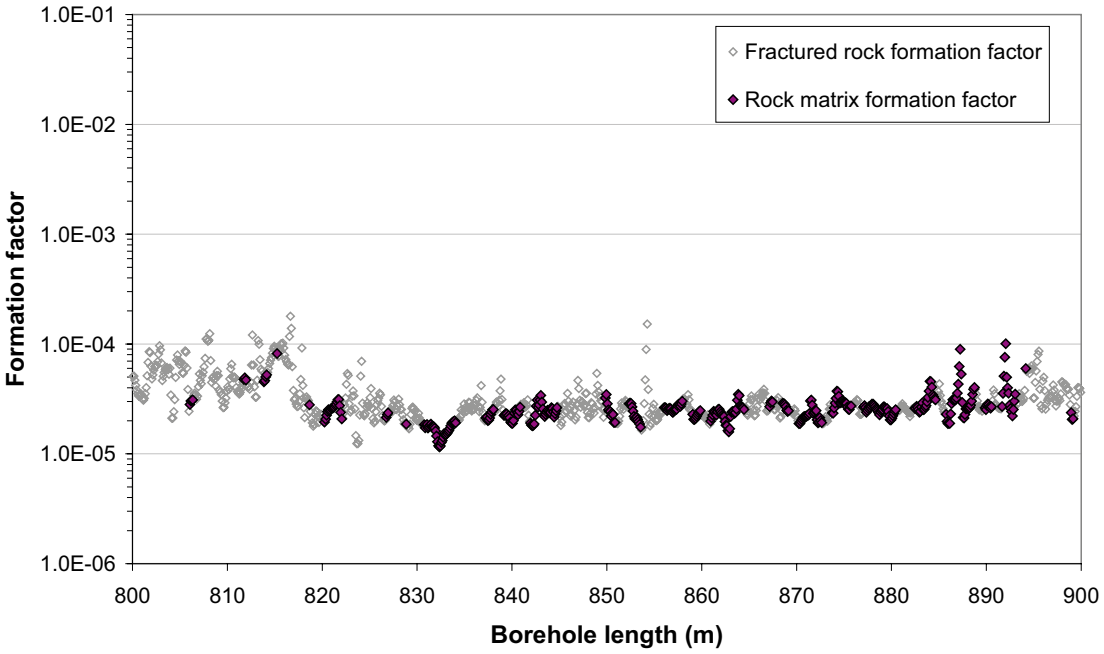
Fractured rock formation factor
Rock matrix formation factor
Formation factor
1.0E-01
1.0E-02
1.0E-03
1.0E-04
1.0E-05
1.0E-06
800
810
820
830
840
850
860
870
880
890
900
Borehole length (m)

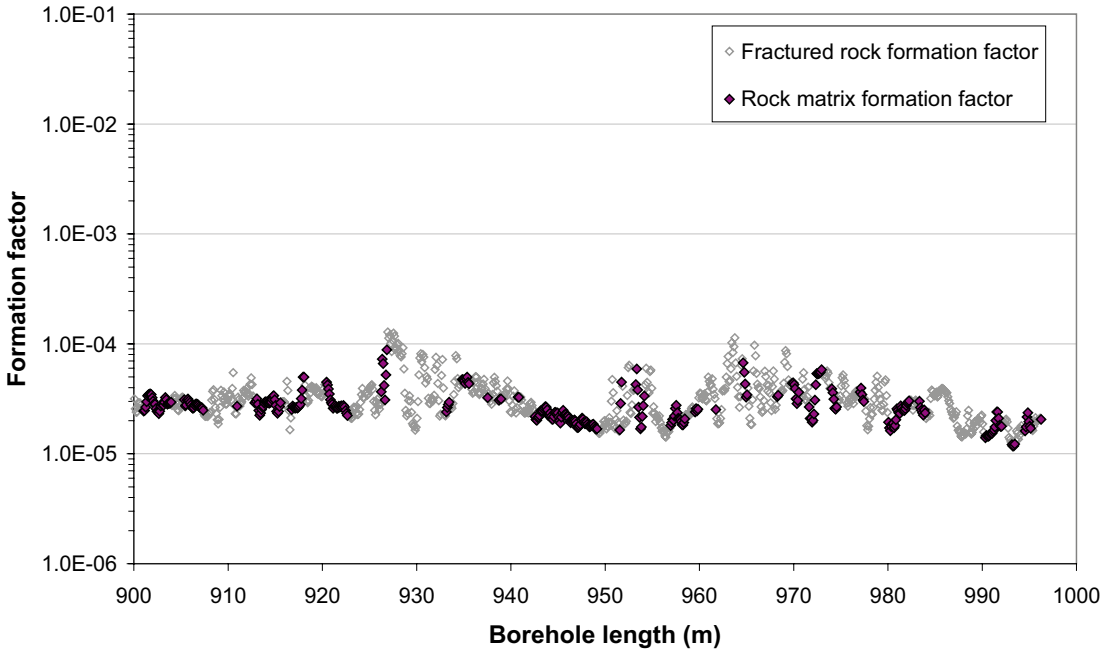
1.0E-01
1.0E-02
1.0E-03
1.0E-04
1.0E-05
1.0E-06
Formation factor
900
910
920
930
940
950
960
970
980
990
1000
Borehole length (m)
Fractured rock formation factor
Rock matrix formation factor

Appendix C3: Comparison of laboratory and in-situ formation factors KFM05A

Borehole length (m)	Laboratory F_f	Rock matrix F_f	Ratio Laboratory/ Rock matrix F_f
208.835	7.09E–05	–	–
228.145	1.39E–04	2.15E–05	6.5
249.045	2.91E–04	–	–
269.675	1.69E–04	2.38E–05	7.1
288.865	1.48E–04	2.81E–05	5.3
308.565	1.61E–04	3.16E–05	5.1
348.265	1.81E–04	3.79E–05	4.8
388.945	1.68E–04	2.38E–05	7.1
408.765	1.36E–04	3.53E–05	3.9
428.95	4.09E–05	–	–
449.365	1.32E–04	4.48E–05	2.9
469.845	3.52E–04	3.92E–05	9.0
489.375	3.57E–04	3.25E–05	11.0
509.085	7.01E–04	4.11E–05	17.1
528.735	1.22E–04	3.25E–05	3.8
548.555	1.39E–04	3.49E–05	4.0
590.065	1.27E–04	2.79E–05	4.6
629.315	2.64E–04	–	–
650.435	1.46E–04	2.22E–05	6.6
669.915	8.17E–05	–	–
689.705	1.13E–04	2.18E–05	5.2
700.295	4.38E–04	2.12E–05	20.7
739.835	2.48E–04	–	–

Laboratory F_f = Formation factor obtained in the laboratory

Rock matrix F_f = Arithmetic mean value of in-situ rock matrix formation factors from within 0.5 m of the borehole length.

Appendix D

Groundwater EC data Forsmark

Borehole	Inclination	Borehole length	Borehole depth	EC 25°C	EC in-situ	Method
KFM01A [1)]	84.7°	116.0	115.5	1.52	1.01	HC
		178.0	177.2	1.55	1.05	HC
KFM02A [1)]	84.7°	110.7	110.2	0.22	0.15	Diff
		111.1	110.6	0.22	0.15	Diff
		112.9	112.4	0.16	0.11	Diff
		114.2	113.7	0.18	0.12	Diff
		116.6	116.1	0.14	0.09	Diff
		117.5	117.0	0.15	0.10	Diff
		118.3	117.8	0.12	0.08	Diff
		119.0	118.5	0.12	0.08	Diff
		120.9	120.4	0.35	0.23	Diff
		121.1	120.5	0.41	0.27	Diff
		162.8	162.1	1.3	0.87	Diff
		171.7	171.0	1.2	0.81	Diff
		426.8	425.0	1.6	1.15	Diff
		513.6	511.4	1.6	1.17	Diff
KFM03A [1)]	85.8°	388.6	387.5	2.34	1.67	Diff
		388.6	387.5	1.65	1.17	Diff
		451.3	450.0	2.28	1.65	Diff
		451.3	450.0	1.63	1.18	Diff
		643.9	642.1	2.28	1.72	Diff
		643.9	642.1	1.62	1.23	Diff
		643.9	642.1	1.61	1.22	Diff
		944.2	941.5	3.29	2.66	Diff
		944.2	941.5	2.31	1.87	Diff
		986.4	983.6	3.84	3.14	Diff
		986.4	983.6	2.89	2.36	Diff
KFM04A [1)]	60.1°	116.3	100.8	0.87	0.58	Diff
		207.1	179.5	1.4	0.95	Diff
		235.6	204.2	1.46	0.99	Diff
		297.1	257.6	1.48	1.02	Diff
		359.8	311.9	1.45	1.01	Diff
KFM05A	59.8°	116.5	100.7	1.56	1.04	Diff
		124.3	107.4	1.54	1.02	Diff
		175.6	151.8	1.44	0.97	Diff
		264.4	228.5	1.41	0.97	Diff
		720.0	622.3	1.38	1.04 [2)]	HC
KFM06A	60.3°	126.0	109.44	1.18	0.78	Diff
		128.7	111.79	1.38	0.91	Diff
		129.2	112.18	1.46	0.97	Diff
		130.3	113.18	1.46	0.97	Diff
		131.9	114.52	1.44	0.96	Diff

135.2	117.43	1.43	0.95	Diff
177.4	154.09	1.51	1.02	Diff
181.1	157.30	1.49	1.00	Diff
218.2	189.53	1.46	0.99	Diff
238.0	206.73	1.48	1.01	Diff
268.6	233.31	1.43	0.98	Diff
269.3	233.91	1.45	0.99	Diff
356.6	309.74	1.17	0.81	Diff
743.3	645.63	1.36	1.03	Diff
355.4	308.70	1.34	0.93 [3)]	HC
770.7	669.43	1.95	1.49 [3)]	HC

[1)] Temperature corrections for borehole KFM01A–KFM04A based on assumption that the temperature profile can be approximated by that of KFM06A. Temperature corrections based on /4/.

[2)] Temperature corrections based on /3/.

[3)] Temperature corrections based on /4/.

Data (25°C) from /19/, /3/, /4/, /6/, and /7/.